**T-PM-Po1** USE OF THE DYE HOECHST 33258 IN A MODIFICATION OF THE BROMODEOXYURIDINE PHOTOLYSIS TECHNIQUE FOR THE ANALYSIS OF DNA REPAIR. B. S. Rosenstein* and R. B. Setlow (Intr. by M. Simon), Biology Dept., Brookhaven National Laboratory, Upton, N.Y. 11973.

A modification of the BrdU photolysis technique[1] used in the measurement of the repair of damage in DNA has been developed employing the bisbenzimidazole dye Hoechst 33258. In the original technique 313 nm light is used to photolyze BrdU incorporated into parental DNA during repair. In the modified procedure cells are treated with 10 μg/ml of the dye in PBS for 10 minutes and due to the broad absorption band (maximum at 356 nm) exhibited by chromatin bound dye, 365 nm light may then be used for the photolysis. The number of breaks in BrdU substituted DNA are proportional to the extent of substitution and to the dose. Approximately 2.1 X $10^{-7}$ breaks/BrdU residue per J/$m^2$ are produced in fully substituted DNA from V79 cells by both 313 nm and 365 nm light with dye. The doses used to produce BrdU photolysis are therefore about the same for the two procedures but the modification has several advantages. 1) 365 nm light is not as strongly absorbed as 313 nm light by many chemical carcinogens and therefore some of the effects produced in unsubstituted, unrepaired DNA by 313 nm light may be avoided. 2) Irradiation times may be reduced because the output at 365 nm of a high pressure mercury arc lamp is about double that at 313 nm. 3) It is possible to use a low pressure "black light" as a source for photolysis because of the similarity of its emission spectrum and the absorption spectrum of the Hoechst dye when bound to chromatin. The latter advantage greatly simplifies the equipment necessary to carry out the BrdU photolysis procedure. (This work was supported by the Department of Energy and BSR is a Fellow in Cancer Research supported by Grant DRG-215-F of the Damon Runyon - Walter Winchell Cancer Fund.)

1. Regan, J. D., R. B. Setlow and R. D. Ley. P. N. A. S. 68: 708, 1971.

**T-PM-Po2** IS THE PHOTOHYDRATION OF 1,3-DIMETHYLURACIL CONCENTRATION DEPENDENT?† Helen G. Sellin* and R. O. Rahn, Biology Division, Oak Ridge National Laboratory, Oak Ridge, TN 37830.

A very careful examination of the quantum yield (ϕ) for photohydration of 1,3-dimethyl uracil (DMU) was made by Burr et al. (1). These workers found approximately a 3-fold decrease in ϕ going from $10^{-3}$ M to $10^{-4}$ M DMU. On the basis of their findings, as well as other values in the literature, they concluded that DMU photohydration is unsuitable as a general secondary actinometer. We have reexamined this problem and find, in contrast to the results of Burr and coworkers, a constant value of ϕ = 13 ± 1 X $10^{-3}$ for DMU concentrations between $10^{-4}$ and $10^{-3}$ M and for irradiation wavelengths between 248 nm and 289 nm. These results are consistent with those reported by Johns (2) and support the use of DMU photohydration to estimate light fluences in the ultraviolet region. (†Research sponsored by the Division of Biomedical and Environmental Research, U.S. Department of Energy, under contract W-7405-eng-26 with the Union Carbide Corporation.)

(1) Burr, J. G., Gilligan, C., and Summers, W. A. Photochem. Photobiol. 24, 483 (1976).
(2) Johns, H. E. Photochem. Photobiol. 8, 547 (1968).

**T-PM-Po3** A COMPARISON OF THE EFFECT OF UV ON RNA AND PROTEIN SYNTHESIS IN NON-DIVIDING POPULATIONS OF DNA EXCISION REPAIR PROFICIENT AND DEFICIENT HUMAN CELL STRAINS. G. J. Kantor and D. R. Hull* Wright State University, Dayton, Ohio 45435.

Human cells cultured in medium containing 0.5% calf serum can be maintained in a non-dividing state for long periods (>1 y) and remain viable. Irradiation of these cultures with reasonably low doses of UV (254 nm) causes cells to detach from the culture vessel surface. The detached cells are not viable. The extent of cell detachment is dose and strain dependent. DNA excision repair deficient cells (XP12BE) are more sensitive than excision repair proficient cells (XP4BE, WI-38, WS-1). Results of experiments measuring the effect of UV on synthesis of RNA ($^3$H-uridine incorporation into RNA) indicate that it caused an immediate depression in the rate of RNA synthesis in all strains examined. A recovery to a control rate occurred in XP12BE populations at doses ≤4 J/$m^2$ and in repair proficient populations at doses ≤20 J/$m^2$. These doses permit >60% survival in the respective populations. No recovery was observed at doses that have a large effect on survival (>4 J/$m^2$ for XP12BE; >40 J/$m^2$ for repair proficient strains). No initial effect on rate of protein synthesis (measured by $^3$H-leucine incorporation) at doses <20 J/$m^2$ was detected. However, in XP12BE populations, a decreased rate first evident at 8-12 h post-UV and prior to any cell detachment, was observed for doses as low as 7 J/$m^2$. This delayed effect was not observed in repair proficient populations. The results are consistent with the hypothesis that the lethal action of UV in arrested cells is one on DNA that leads to an inhibition of required protein synthesis by preventing RNA transcription. Removal of DNA damage by excision repair can to a limited extent prevent this inhibition. (Supported by NIH grant CA-16477; present address: Biology Department, Brookhaven National Laboratory, Upton, N. Y. 11973).

**T-PM-Po4** A NONRADIOACTIVE ASSAY FOR THYMINE DIMERS IN UV-IRRADIATED DNA.† Susan S. Chang* and R. O. Rahn (Intr. by W. E. Masker), Biology Division, Oak Ridge National Laboratory, Oak Ridge, TN 37830.

A procedure has been developed whereby thymine containing dimers can be assayed for in nonradioactively-labeled DNA. Irradiated DNA was hydrolyzed in strong acid and the thymine containing dimers separated from the rest of the bases on WA-2, Reeve Angel ion-exchange paper (Brown and Holt, 1967), using 0.1 M acetic acid adjusted to pH 4.8 as a solvent. Since the dimer peak is located closer to the solvent front than thymine, the problem of thymine streaking into the dimer region is eliminated. Elution of both the dimer and thymine fractions from the paper was easily accomplished, using water as a solvent. The dimer fraction was monomerized back to the free bases using 254 nm radiation and the thymine content analysed for, using the fluorescence assay developed by Roberts and Friedkin (1958). In this assay, thymine is degraded to acetol, using a combination of bromination and alkali. The acetol is then condensed with O-aminobenzaldehyde to form the fluorescent derivative 3-hydroxyquinaldine. The sensitivity of the assay currently is such that a 1% yield of dimers in 0.5 mg of DNA can be readily detected. (†Research sponsored by the Division of Biomedical and Environmental Research, U.S. Department of Energy, under contract W-7405-eng-26 with the Union Carbide Corporation.)

Brown, R. D., and Holt, C. E. Anal. Biochem. 20, 358-360 (1967).
Roberts, D., and Friedkin, M. J. Biol. Chem. 233, 483 (1958).

**T-PM-Po5** THE EFFECT OF HYDROXYUREA ON DNA REPAIR IN UV-IRRADIATED HUMAN CELLS.† Andrew A. Francis and James D. Regan,* Biology Division, Oak Ridge National Laboratory, Oak Ridge, TN 37830.

Hydroxyurea (HU) has been used clinically as an antineoplastic drug and as a biochemical tool to inhibit semiconservative DNA synthesis. The effect on DNA repair in UV-irradiated human skin fibroblasts by HU has been examined in this study, using three independent methods for measuring DNA repair: the 5-bromodeoxyuridine photolysis assay which measures DNA repair replication, chromatographic measurement of thymine containing dimers and measurement of specific UV endonuclease sensitive sites in irradiated DNA. Little effect of HU was observed at the concentration of 2 mM which is often used to inhibit semiconservative DNA synthesis; however, at 10 mM the 5-bromouridine photolysis assay indicated a 65 to 70% inhibition of repair synthesis had occurred. This inhibition was accompanied by a possible doubling in the size of the repaired region. A similar reduction in DNA repair was seen when measuring the disappearance of thymine containing dimers from the DNA of irradiated cells chromatographically. Measurement of DNA repair utilizing specific UV endonuclease was less sensitive to HU. An accumulation of single-strand breaks in large numbers following UV irradiation and HU incubation was not observed. A comparison of HU effects on the different DNA repair assays indicates inhibition of one step in DNA repair also results in varying degrees of inhibition of other steps as well. (†Research sponsored jointly by NASA and by NCI under Interagency Agreements # 40-565-76 and # 40-5-63, respectively, and by the Division of Biomedical and Environmental Research, U. S. Department of Energy, under contract W-7405-eng-26 with the Union Carbide Corporation.)

**T-PM-Po6** THE EFFECT OF ARABINOFURANOSYL CYTOSINE (ara-C) ON PYRIMIDINE DIMER INCISION AND EXCISION IN THE DNA OF UV-IRRADIATED NORMAL SKIN FIBROBLASTS.† W. L. Carrier, D. P. Smith,* and J. D. Regan,* Biology Division, Oak Ridge National Laboratory, Oak Ridge, TN 37830.

With ara-C present in the growth media after UV-irradiation, human skin fibroblasts incorporate ara-C into the region of dimer repair. The results are incomplete repair as shown by the accumulation of single-strand breaks in the DNA.[1,2] We have found that ara-C inhibits the excision of pyrimidine dimers from the DNA of UV-irradiated normal skin fibroblasts. Dimers were measured by two-dimensional paper chromatography.[3] With ara-C present, a maximum of 20% of the dimers were excised in the first six hours after UV. Control cells excised approximately 90% within 48-72 hours. A dose of 20 J/m$^2$ of 254 nm UV light produces 78 UV-specific endonuclease sensitive sites (ESS) in $10^8$ daltons of DNA. The sites equaled the number of dimers and were observed by alkaline sucrose sedimentation analysis of the DNA. During repair control cells removed about half (38) of the ESS in 24 hours, and this was accompanied by other repair steps (i.e., excision, resynthesis, rejoining). Fewer sites were removed from ara-C-treated cells during this period. Also, the ESS removal (incisions) that did occur were not accompanied by other repair steps. This resulted in small DNA observed upon sedimentation in alkali. (†Research sponsored by the Division of Biomedical and Environmental Research, U. S. Department of Energy under contract W-7405-eng-26 with the Union Carbide Corporation.)

1. Johnson, R. T. and Collins, A. R. S., Biochem. Biophys. Res. Commun. 80, 361-369 (1978).
2. Dunn, W. C. and Regan, J. D., Mol. Pharmacol., in press (1979).
3. Carrier, W. L. and Setlow, R. B., Meth. Enzymol. XXI, Part D, 230-237 (1971).

**T-PM-Po7** LESIONS INDUCED IN DEOXYRIBONUCLEIC ACID BY BENZO[*a*]PYRENE AND NEAR ULTRAVIOLET LIGHT. G.F. Strniste, A.M. Martinez* and E.M. Martinez,* Cellular and Molecular Biology Group, Los Alamos Scientific Laboratory, The University of California, Los Alamos, New Mexico 87545 U.S.A.

Superhelical PM2 DNA (form I) was mixed with benzo[*a*]pyrene (B[*a*]P) at a mass ratio of 10:1 (DNA:B[*a*]P) and exposed to near ultraviolet (uv) light (300-500 nm). Both neutral and alkali sucrose gradients were performed and the rates of single-strand breaks induced in the DNA were determined by monitoring the conversion of form I to the open, relaxed circular form of PM2 DNA (form II). Single-strand breaks (under neutral conditions) were induced 12.5 to 14 X as rapidly by the radiation in the presence of B[*a*]P compared to breaks induced in the absence of B[*a*]P. The rate of single-strand breaks observed under alkali conditions was 2-3 X the rate observed under neutral conditions. Using molecular sieve column chromatographic methods it was possible to determine the amount of [$^{14}$C]B[*a*]P which co-eluted with the [$^{3}$H]PM2 DNA as a function of radiation exposure. In an argon-saturated environment, there existed 11 B[*a*]P molecules per PM2 DNA molecule per single-strand break (neutral) whereas in an oxygen-saturated environment, there existed approximately 14 B[*a*]P molecules per PM2 DNA molecule per single-strand break (neutral). Isolated PM2 DNA-B[*a*]P adducts which were enzymically digested and chromatographed on Sephadex LH-20 revealed at least 5 distinct peaks eluting through a 30-100% methanol:water gradient. These peaks have been isolated and are being examined by gas chromatographic-mass spectrophotometric methods. (This work was performed under the auspices of the U. S. Department of Energy.)

**T-PM-Po8** EFFECT OF ACETOXYACETYLAMINOFLUORENE ON TRANSFECTION OF *E. COLI* BY ΦX-174 RF-DNA. W. D. Taylor, R. A. Deering, and C.-L. Tsai*, The Pennsylvania State University, University Park, PA 16802

Acetoxyacetylaminofluorene and near UV (303 nm) inactivate the transfecting activity of ΦX174 RF-DNA on calcium treated *E. coli* at carcinogen concentrations in the range 1-10 μgm/ml and doses in the range 1-2 X $10^{5}$ ergs/mm$^{2}$, and the combined treatments have a synergistic effect. No single or double-strand breaks are observed by neutral sucrose gradient sedimentation. Alkali-labile bonds and $S_1$ nuclease sensitive sites are found but much less frequently than inactivating nucleotide damage. Using *E. coli* repair mutants, it was found that the *uvrA* gene is involved in the repair of this damage. (Supported by the National Institutes of Health).

**T-PM-Po9** HOST CELL REACTIVATION OF *B. SUBTILIS* BACTERIOPHAGES Φ29 AND SPO2-c12. W. L. Pepper* and L. L. Larcom, Depts. of Microbiology and Physics, Clemson University, Clemson, S. C. 29631.

Bacillus subtilis strains RUB818 (uvr$^{+}$) and YB864 (uvr$^{-}$) were used as hosts for irradiated bacteriophages φ29 and SPO2-c12. Linear survival curves (log surviving fraction versus dose) were obtained for both phages in each host. The slope of the survival curve was used as an inactivation constant. Phage SPO2-c12 had inactivation constants of -2.65x$10^{-3}$ mm$^{2}$/erg in strain RUB818 and -19.9x$10^{-3}$ mm$^{2}$/erg in strain YB864. Phage φ29 had inactivation constants of -2.87x$10^{-3}$ and -20.0x$10^{-3}$ mm$^{2}$/erg, respectively. When either bacterial strain was irradiated prior to phage infection, the inactivation constant became less negative for both phages studied. However, when host cells were infected with highly irradiated φ29 and subsequently used as recipient cells for SPO2-c12 infection, the inactivation constant obtained for UV-irradiated SPO2-c12 was the same as that obtained using untreated host cells as recipients. Similar results were obtained when cells pre-infected with highly irradiated SPO2-c12 were used to assay the survival of UV-irradiated φ29. These results indicate that although there is probably an inducible dark repair system in *B. subtilis* similar to that present in *E. coli*; the presence of UV-damaged extrachromosomal DNA is not sufficient to induce this system.

T-PM-Pol0 TERTIARY STRUCTURAL COLLAPSE OF DNA IN 5.5 M LiCl INFERRED FROM QUASIELASTIC LIGHT SCATTERING. N. Parthasarathy,* K.S. Schmitz, Dept. Chemistry, Univ. Mo.-Kansas City, Mo. and M. Cowman, Grad. Dept. Biochemistry, Brandeis Univ., Waltham, Mass.

Sedimentation velocity and quasielastic light scattering (QLS) methods have been employed to determine the extent of DNA tertiary structure alteration in 5.5 M LiCl as a possible explanation of the C-form circular dichroism (CD) spectrum. The QLS experiments suggest DNA data can be interpreted in terms of the Lin-Schurr theory for flexible Rouse-Zimm polymers, i.e. the reciprocal relaxation time ($1/\tau$) plotted as a function of $\sin^2(\theta/2)$ exhibits two linear regions reflecting the values of $D_t$ (translational diffusion coefficient, low angle) and $D_s$ (segmental diffusion coefficient, high angle). The Stokes radius estimated from $D_t$ in 0.4 M $NH_4Ac$ and 5.5 M LiCl is 228 nm and 110 nm, respectively. The difference in the CD spectra for DNA in these two solvent systems is a single negative band, centered at 275 nm, which is qualitatively identical to the spectrum observed for condensed ψ-DNA structure. These data suggest a partial collapse of the DNA tertiary structure in 5.5 M LiCl which emphasizes the care that must be exercised in the interpretation of CD spectra. This research was supported in part by grants from NSF (PCM 7622073 (KSS)) and NIH (GM 24346 (KSS) and GM 17533 (MC)).

T-PM-Pol1 PYRIMIDINE (3'-5') PURINE BASE SEQUENCE PREFERENCE FOR INTERCALATION INTO RNAS† S. Broyde, Biology Dept., New York University, N.Y., N.Y. 10003 and B. Hingerty, Biology Division, Oak Ridge National Laboratory, Oak Ridge, Tenn. 37830.

Experimental crystal structures and solution studies indicate that planar aromatic molecules prefer to intercalate into pyrimidine (3'-5') purine base sequences of RNAS. Recent work (1) has shown that increases in the glycosidic torsion, χ and the C5'-O5' torsion, φ , are the major conformational changes common to intercalated crystal structures. We have calculated energy contour maps in the χ, φ plane for UpA and GpC. These reveal that in the RNA-11 A form, the pyrimidine (3'-5') purine base sequence has a much larger low energy conformation space for χ than the reverse sequence. This is due to the diminished base stacking in the former. Consequently, where intercalation into A forms occurs by increases in χ and φ, the pyrimidine (3'-5') purines are preferred over the purine (3'-5') pyrimidines, although the preference is to the extent of only 5 kcal./mole.

(1) Berman, H., Neidle, S. and Stodola, R. (1978) Proc. Nat'l. Acad. Sci. USA 75, 828-832

† Research supported jointly by NIH Grant # 2ROGM24482-2 awarded to SB and the Division of Biomedical and Enviromental Research, U.S. Dept. of Energy under contract W-7405-eng-26 with the Union Carbide Corp.

T-PM-Pol2 RIFAMPICIN AS A SPECTROSCOPIC PROBE OF THE MECHANISM OF E. COLI RNA POLYMERASE. R. Reisbig,* A-Y.M. Woody,* and R.W. Woody, Department of Biochemistry, Colorado State University, Fort Collins, CO. 80523.

Rifampicin, a potent inhibitor of prokaryotic RNA polymerase, has several absorption bands at wavelengths longer than 300 nm, making it a potentially useful absorption and CD probe of RNA polymerase. The hydroquinone form of rifampicin, which is most widely used in inhibition studies, undergoes fairly rapid oxidation in various aqueous buffers, especially Tris, to the quinone form. We have determined the CD and absorption spectra of both forms free in solution and in complexes with RNA polymerase. Both optical properties show substantial changes when rifampicin, oxidized or reduced, binds to the enzyme. A red shift in the absorption spectrum of rifampicin and the resistance to oxidation of the reduced rifampicin-RNA polymerase complex imply that the substituted naphthalene chromophore of rifampicin is buried in the complex. Within experimental error, the changes in absorption and CD were identical for binding to holoenzyme and core polymerase. Small changes in the rifampicin CD are observed when poly(dT) is added to the rifampicin-enzyme complex. Large changes in the difference spectrum are observed when poly(dT), ApA and ATP are added. This may be evidence for a significant conformational change in the enzyme before the first elongation step. (Supported in part by NIH Grant GM 23697.)

**T-PM-Pol3** Carbon-13 NMR Study on Deoxyribodinucleoside Methyl Phosphonates. J. Yano*, P.S. Miller*, D. Cheng*, P.O.P. Ts'o and L.S. Kan, Div. of Biophysics, Johns Hopkins University, Baltimore, MD 21205.

The stacking interaction of the two diastereoisomers of dAOP(O)($CH_3$)OdA are slightly different in aqueous solution (Biophys. J. 21, 112a (1978)). In order to study the backbone conformation of the dimers we have synthesized and separated both the pseudoaxial (isomer 1) and the pseudoequitorial (isomer 2) isomers of dAOP(O)($^{13}CH_3$)OdA (95% carbon-13). The chemical shifts of all carbons were assigned according to dApdA (J.L. Alderfer, private communication). In general, the chemical shifts of isomer 1 are more upfield shift than that of isomer 2. This result agrees with the previous pmr result and shows that isomer 1 is more stacked than isomer 2. Based on stacked models of these dimers, dihedral angles are formed by $CH_3$-P-O and P-O-$C_3$' ($\sim 30^o$ in isomer 1 and $\sim 150^o$ in isomer 2) and by $CH_3$-P-O and P-O-$C_5$' ($\sim 160^o$ in isomer 1 and $\sim 90^o$ in isomer 2). However, the coupling constants between $CH_3$-$C_3$' (dAp-) and $CH_3$-$C_5$' (-pdA) are 0 and less than 2 Hz, respectively. This indicates that the coupling constants are insensitive to changes in rotation about $\omega$ and $\omega$'. The $J_{P-C4'}$ of isomer 1 (7 Hz) does not change with increasing temperature while that of isomer 2 increases from 4.4 Hz ($15^o$) to 7.3 Hz ($40^o$). Thus rotation about $\phi$ is less restricted in isomer 2, which is in agreement with previous results. Thus, the differences in base stacking between isomer 1 and isomer 2 are explained by changes in the rotation about $\phi$ and $\psi$. These changes could be caused by differences in solvation of the two isomers. Supported by NSF and NIH.

**T-PM-Pol4** COMPARISION OF THE STACKING PATTERNS BETWEEN ADJACENT BASE-PAIRS IN DOUBLE-HELICAL NUCLEIC ACIDS: A GRAPHICAL APPROACH. Chun-che Tsai, S. C. Kao*, and C. G. Reinhardt, Department of Chemistry, Kent State University, Kent, Ohio 44242.

Structural and geometrical analyses, based on the stereochemical information deduced from the existing X-ray diffraction data of nucleic acids in fibers and crystals, have been applied to investigate the base-pair stacking pattern between adjacent base-pairs in double-helical nucleic acids. The base-pair stacking patterns can be described by parameters such as angular twist between adjacent base-pairs, the orientation and position of base-pair with respect to adjacent base-pairs, and the angle between adjacent base-pair planes. A correlation between DNA-kinking angle and the double-helical parameters (such as axial translation, pitch and tilt angle) has been derived, which suggests the existence of DNA-kinking in various forms of DNA and polynucleotide structures (A-, B-, C- and D-forms) as deduced from X-ray diffraction analysis of DNA and polynucleotide fibers. A graphical approach for comparing the stacking patterns between adjacent base-pairs with different base sequences in double-helical nucleic acids has been developed which may be used to estimate the ring-current effects in the NMR of double-helical nucleic acids. (Supported by NIH grant GM 24259).

**T-PM-Pol5** HIGH AFFINITY AND MULTIPLE-SITE BINDING OF BIFUNCTIONAL INTERCALATING DIMERS TO YEAST $tRNA^{phe}$. Christian G. Reinhardt, [+]Laboratoire de Physicochimie Macromoléculaire, Institut Gustave-Roussy, 94800 Villejuif, France.

The fluorescence properties and tRNA binding interactions of a recently synthesized ethidium homodimer and an acridine-ethidium heterodimer (1) have been investigated. Fluorescence titration, lifetime, energy transfer, stopped-flow kinetic and equilibrium dialysis measurements on the binding of these compounds to yeast $tRNA^{phe}$ indicate from 1 to 3 high-affinity fluorescent dimer binding sites per tRNA molecule with association constants exceeding $10^9$ $M^{-1}$, in addition to multiple lower-affinity binding sites. The mode of binding appears to involve both intercalated and electrostatically bound non-intercalated dimer species as evidenced by the fluorescence enhancement and fluorescence lifetimes of the dimers bound to tRNA, as well as by measurements of the efficiency of energy transfer from tRNA bases to the bound dimers. Variations in the stoichiometry of the dimer-tRNA complexes as a function of ionic strength and $Mg^{++}$ ion concentration, cooperative type binding between high and lower-affinity binding sites and the observation of several distinct kinetic relaxation processes suggests a complex binding mechanism which may be sensitive to, or coupled with, conformational changes within the macromolecule. Possible biological implications of the binding of these bifunctional intercalating dimers to tRNA and the potential utility of these compounds as fluorescence probes to tRNA structure and function will be discussed. (Supported by an NSF-CNRS Exchange Fellowship).

(1) Gaugain, B., Barbet, J., Oberlin, R., Roques, B. P., and Le Pecq, J.-B. (1978) Biochemistry 17, in press.

[+] Present Address: Department of Chemistry, Kent State University, Kent, Ohio 44242

**T-PM-Pol6** HYDROGEN AND CARBON NMR STUDIES ON THE CONFORMATION OF NUCLEIC ACIDS CONTAINING 4'-THIO-FURANOSE. J.L. Alderfer, J.D. Bloss*, and G. Hazel*, Department of Biophysics, Roswell Park Memorial Institute, Buffalo, New York 14263.

Nucleic acid constituents which have the furanose ring oxygen (C4'-O-C1') exchanged for a sulfur atom (C4'-S-C1') are biologically active, and exhibit antitumor activity. Chemical shifts ($^1H$, $^{13}C$) and coupling constants (H-H, C-P, C-H) of nucleosides and nucleotides are determined for these sugar analogs of uracil and guanine. The effects of sulfur substitution on the $^1H$ chemical shifts are mainly on H4' (0.67 ppm upfield) and H6 (0.27 ppm downfield), while for $^{13}C$ chemical shifts, large upfield shifts of C1' (20 ppm), C4' (30 ppm), and downfield shifts of C2', C3', C5' and C6 are observed. Conformational populations obtained from coupling constants of normal and 4'-thio-derivatives are (0.1 M/$D_2O$, 27°): (1) Urd, C2'-endo (0.45), C3'-endo (0.55); $\psi$: $g^+$ (0.66), $g^-$ (0.24), t (0.10); (2) (4'-S)Urd, C2'-endo (0.55), C3'-endo (0.45); $\psi$: $g^+$ (0.34), $g^-$ (0.37), t (0.29); (3) 5'-UMP, C2'-endo (0.54), C3'-endo (0.46); $\psi$: $g^+$ (0.89), $g^-$(0.08), t (0.03); $\phi$: t (0.77), $g^+$ (0.11), $g^-$(0.17); (4) 5'-(4'-S)UMP, C2'-endo (0.61), C3'-endo (0.39); $\psi$: $g^+$ (0.48), $g^-$ (0.31), t (0.21); $\phi$: t (0.64), $g^+$ (0.17), $g^-$ (0.19); (5) $Ac_4$-(4'-S)-N7-Guo, C2'-endo (0.70), C3'-endo (0.30) $\psi$: $g^+$ (0.00), $g^-$ (0.41), t (0.59); (6) 5'-GMP, C2'-endo (0.62), C3'-endo (0.38), $\psi$: $g^+$ (0.72), $g^-$ + t (0.28); $\phi$: t (0.72), $g^+$ + $g^-$(0.28); (7) 5'-(4'-S)-N7-GMP, C2'-endo (0.38), C3'-endo (0.62); $\psi$: $g^+$ (0.37), $g^-$ (0.35), t (0.28); $\phi$: t (0.63), $g^+$ (0.20), $g^-$ (0.17). The sugar-base coupling constants ($^3J_{H1',C2}$, $^3J_{H1',C6}$) are related to the dihedral angle, $\chi$(C1',N); these values are similar in Urd and (4'-S)Urd, indicating similar average values of $\chi$. The main conformational effects of sulfur substitution shown by these results are a shift of the furanose conformation toward more C2'-endo forms, destabilization of the $g^+$ rotomer of $\psi$(C4'-C5'), and destabilization of the t rotomer of $\phi$(C5'-O5').

**T-PM-Pol7** CONFORMATION WHEELS: A NOVEL PROBE OF tRNA FOLDING. A. R. Srinivasan and W. K. Olson, Chemistry Dept., Douglass College, Rutgers, The State University, New Brunswick, N. J. 08903.

A series of conformation wheels has been constructed from the recently refined X-Ray crystallographic data of both the monoclinic[1] and the orthorhombic[2] forms of yeast $tRNA^{Phe}$. These circular plots relate the primary chemical structure (i.e., base sequence) directly to the secondary and tertiary structure of the molecule. The circular sequence of backbone torsion angles displays a unique pattern that is useful both in distinguishing the ordered and disordered regions of the molecule and in comparing the two sets of experimental data. Additional plots of the base stacking and backbone helical parameters of individual residues help to visualize the intimate interrelationship between chemical sequence and three-dimensional folding in the polynucleotide backbone. Several categories of bends appear in these latter wheels. Interestingly, a number of "left-handed" helix promoting sequences occur in the four right-handed helical stems of the molecule. The irregularity of the helical stems also provides information relevant to the superhelical bending of RNA.

(1) Hingerty, B., Brown, R. S. and Jack, A. (1978) J. Mol. Biol. (in press).
(2) Sussman, J. L., Holbrook, S. R., Warrant, R. W., Church, G. M., and Kim, S. H. (1978) J. Mol. Biol., 123, 607-630.

**T-PM-Pol8** COMPUTER ANALYSIS OF ESR SPECTRA OF SPIN LABELED NUCLEIC ACID LIGAND COMPLEXES. A. M. Bobst, T. Sinha*, P. W. Langemeier*, Chemistry 172, University of Cincinnati, Cincinnati, OH 45221.

A saturation parameter F is determined to measure the degree of binding of amino acid containing ligands (L) to a spin labeled nucleic acid matrix. A program FDET was written to get F utilizing the entire ESR spectra. FDET requires as input 3 data sets of properly aligned ESR spectra: $C_s$ spectrum of ligand saturated spin labeled nucleic acid matrix, $L \geq L_s$; $C_o$ spectrum with L = 0; C spectrum with $L < L_s$, L > 0. The ESR spectra were digitally aligned by searching for the addresses of the 2nd crossover point (CRO) since for the systems studied it was experimentally established that the position of the 2nd CRO of the nitroxide spectrum remains unchanged relative to the position of the CRO of the external $Cr^{3+}$ standard. A partially saturated spin labeled nucleic acid system is analyzed according to $D = C - F \cdot C_s - (1-F) \cdot C_o$. Titrating spin labeled $(U)_n$ with poly-L-lysine gave C spectra which seem to indicate the presence of a two component system of saturated and free lattices since at certain F values the difference spectrum D was a straight line. Supported in part by NIH grant CA 15717.

**T-PM-Po19** THERMAL DENATURATION RESULTS OF DNA RESTRICTION FRAGMENTS.
D. L. Vizard and A. T. Ansevin, Department of Physics, University of Texas System Cancer Center, M. D. Anderson Hospital and Tumor Institute, Texas Medical Center, Houston, TX 77030.

The multi-modal thermal derivative denaturation patterns of bacteriophage and viral DNAs can be viewed as a sum of a series of thermal transition elements (thermalites). However, the deconvolution of such a derivative profile for even a small viral DNA tends to seriously under-estimate the number of thermalites actually present in the profile. It is necessary to minimize the ambiguities arising from the presence of cryptic thermalites so that the variation of denaturation profiles with pH, salt, or denaturant can be adequately studied. The much less complex denaturation patterns obtained from restriction fragments of viral genomes can alleviate much of the ambiguity associated with the deconvolution of profiles. We now have available derivative profiles for restriction fragments from a variety of viral DNAs, many of which have been denatured at various salt concentrations. We have also studied the variation of some fragment patterns as a function of denaturant concentration and pH. Among the restriction fragments we have studied are selected fractions of the SV-40 genome, which afford the opportunity to compare the thermal denaturation results with features of the primary sequence. Supported by N.I.H. Grant GM 23067.

**T-PM-Po20** LIGHT SCATTERING PERTURBATIONS ON THE MEASUREMENT OF THE OPTICAL ACTIVITY OF LARGE PARTICLES. M.F. Maestre, Donner Laboratory, University of California, Berkeley California 94720.

By application of such techniques as Fluorescence Detected Circular Dichroism (FDCD) and large angle acceptance methods in CD (Fluorscat cuvettes, large area photo multipliers, beam goniometers) we have been able to measure the circular dichroism scattering components of a variety of interesting biological materials. These materials include viruses, chromosomes, intact cell nuclei, DNA histone aggregates, polylysine-DNA complexes and DNA films. From these measurements we have determined that most of the strikingly large magnitudes of the CD of some of these types of particles are a manifestation of scattering perturbations and that their polarization properties reflect the large scale organization of the particles.

**T-PM-Po21** APPLICATION OF RAMAN SPECTROSCOPY AS A STRUCTURAL PROBE OF RIBOSOMES AND RIBOSOMAL SUBUNITS. M.G. Hamilton, Sloan-Kettering Institute for Cancer Research, New York, NY 10021, and B. Prescott* and G.J. Thomas, Jr., Department of Chemistry, Southeastern Massachusetts University, North Dartmouth, MA 02747.

Using 514.5 nm excitation of an argon ion laser, Raman spectra of high signal-to-noise quality have been obtained on ribosomes, ribosomal subunits and unfractionated rRNA from both E. coli and rat liver (RL) cells. Spectra were obtained, depending upon sample solubility, from either $H_2O$ and $D_2O$ solutions or pellets, all at 5°C. The Raman spectra show that the ribosomal particles contain highly ordered rRNA molecules in which most of the bases exist in regions of ordered A-helical structure. In 1 mM $MgCl_2$, RL ribosomes contain rRNA that is 78 ± 6% ordered. In 3 mM $MgCl_2$, E. coli ribosomes contain rRNA that is 88 ± 6% ordered. Neither type of rRNA is significantly changed in the amount of ordered structure after extraction from its respective ribosomal subunits. No structural changes are evident in rRNA within a given ribosome when the $Mg^{2+}$ concentration is varied in the range 0 to 5 mM. The weight percent compositions of protein in different ribosomal subunits (i.e., 30% in E. coli 30S and 50S, 45% in RL 60S, and 55% in RL 40S subunits) are revealed in the Raman intensities of specific lines (ca. 2950, 1447, and 1003 $cm^{-1}$) due to vibrations of protein residues. However, firm conclusions about the protein chain conformations in intact ribosomes cannot be reached from the Raman spectra because of the relatively low Raman intensities of the proteins in intact ribosomes. The Raman spectrum of the total protein extracted from RL ribosomes gives evidence of little ordered secondary structure.

Supported by Grants CA 17085-03 (M.G.H.) and AI 11855-04 (G.J.T., Jr.).

**T-PM-Po22** MULTISTATE MODEL FOR THE RANDOM COIL FORM OF POLY(rU).† B. E. Hingerty, Biology Division, Oak Ridge National Laboratory, Oak Ridge, TN 37830 and S. Broyde, Biology Department, New York University, New York, NY 10003.

A multistate model has been constructed from the minimum energy conformers of UpU that reproduces the characteristic ratio ($C_\infty$) of 17 to 18 of poly(rU) (1) and the NMR data (2). The minimum energy conformations were computed by semiempirical methods and the areas in the $\omega',\omega$ maps were obtained by varying $\omega$ and $\omega'$ in 1° intervals, keeping other angles fixed, which locates the 1 kcal/mole wall. The model consists of the following conformers: (1) 36% $\omega',\omega$ = t,$g^-$, C3' endo; (2) 47% $\omega',\omega$ = t,$g^-$, C2' endo and (3) 17% $\omega',\omega$ = $g^-$,t; $\psi$ = t (Watson-Crick) C3' endo. No A form was found to be necessary. The persistence vector calculated by the method of Olson (3) has magnitude $|a|$ = 25.2 A° with components (17.2, -18.4, 0.8) making angles with the x, y and z axes of 46.8°, 136.8° and 88.3°. It is primarily orthogonal to the z axis. This model matches the NMR data that requires 47% C2 endo, 53% C3' endo and 17% $\psi$ = trans. This is the only multistate model that reproduced $C_\infty$ and the NMR data. An earlier two state model matched $C_\infty$ and $|a|$ with 92% A form and 8% $\omega',\omega$ = t,$g^-$, C2' endo but did not match the NMR data. Other two state models were developed that matched $C_\infty$ but not the NMR data. (†Research sponsored jointly by the National Institutes of Health, Grant Number 2ROGM24482-02, and the Division of Biomedical and Environmental Research, U. S. Department of Energy under contract W-7405-eng-26 with the Union Carbide Corporation.)

(1) L. D. Inners and G. Felsenfeld, J. Mol. Biol. (1970) 50, 373-389.
(2) C. H. Lee, F. S. Eyra, N. S. Kondo, R. H. Sarma and S. S. Danyluk, Biochemistry (1976) 15, 3627-3639.
(3) W. Olson, "Flexible DNA Double Helix. I" (in press).

**T-PM-Po23 PATTERNS IN THE NUCLEOTIDE SEQUENCES OF VIRAL GENOMES.** R.M. Schwartz and M.O. Dayhoff, Nat. Biomed. Res. Fnd., Georgetown Univ. Med. Ctr., 3900 Reservoir Rd., N.W., Washington, D.C. 20007

We have developed a computer program that determines which doublets or triplets in a nucleotide sequence occur with frequencies that differ significantly from their expected values based on nucleotide composition. We have used this program to analyze both the complete sequences and the protein-coding portions of the genomes of SV40, ØX174, and MS2, and the complete sequence of potato spindle tuber viroid (PSTV). Doublets that occur with unexpectedly high or low frequency can be assigned an additional factor that corrects for this. The mininmum number of factors sufficient to explain the observed pattern in doublet frequencies is determined. Unusual doublet frequencies have a pronounced effect on the triplet frequencies to be expected, and we have estimated the extent to which patterns in the triplet frequencies can be explained on this basis. Significant patterns in the triplets may also be due to patterns in the codons. As a basis for comparison with the protein-coding portions of these sequences, we generated by computer, sequences that specify the known protein sequences but whose codons are selected at random from those specifying each amino acid. Patterns in the doublets and triplets of the computer generated sequences provide an estimate of the order imposed on the genome by the proteins it codes. The remaining pattern in these nucleotide sequences may be the result of constraints of replication, of transcription, and of secondary structures formed by the sequences of ØX174, MS2, and PSTV or the mRNAs specified by the SV40, ØX174, and MS2 sequences. (Supported by NASA contract NASW-3130 and NIH grant GM-08710).

**T-PM-Po24** MECHANISM FOR THE BINDING OF CIS- AND TRANS-DICHLORODIAMMINE Pt(II) (DDP) TO DNA.† N. P. Johnson, J. D. Hoeschele,*† and R. O. Rahn, Biology Division and Health and Safety Research Division,† Oak Ridge National Laboratory, Oak Ridge, TN 37830.

cis-DDP is an antitumor drug whose activity is believed to be a result of binding to DNA. The trans isomer is inactive. We have studied the reaction of these compounds with DNA *in vitro* to see if the biological activity is correlated with their ability to bind to DNA. We have measured the kinetics of binding for the aquated species trans-$[Pt(NH_3)_2Cl(H_2O)]^+$, cis-$[Pt(NH_3)_2(H_2O)_2]^{+2}$, and cis-$[Pt(NH_3)_2Cl(H_2O)]^+$. The neutral species, trans-$[Pt(NH_3)_2Cl(OH)]$, cis-$[Pt(NH_3)_2(OH)_2]$, and cis-$Pt[(NH_3)_2Cl(OH)]$ are unreactive at low DDP/DNA ratios. In aqueous solution cis-DDP undergoes two distinct reactions, a fast reaction due to cis-$[Pt(NH_3)_2(H_2O)_2]^{2+}$ and a slow reaction due to cis-$[Pt(NH_3)_2Cl(H_2O)]^+$. The monochloro-monoaquo species binds by two pathways, loss of $Cl^-$ to form the diaquo species and direct reaction with the DNA. Binding to DNA is quantitative and irreversible for both compounds, indicating that, unlike many metals, covalent interactions with DNA are responsible for the biological effects. Although there are some differences in the kinetics of binding for the two isomers, under biological conditions (pH 7, 0.15 M NaCl) both bind to DNA to the same extent during 24 hours.

†Research sponsored by the Division of Biomedical and Environmental Research, U. S. Department of Energy under contract W-7405-eng-26 with the Union Carbide Corporation.

**T-PM-Po25** DNA STRAND SPECIFICITY IN THE INTERACTION OF RNA POLYMERASE WITH T7 DNA. C.S. Park*, Z. Hillel, and C.-W. Wu, Biochemistry Dept., Albert Einstein Col. Medicine, Bronx,N.Y. 10461.

The strand specificity in the interaction between the subunits of E. coli RNA polymerase and T7 DNA was investigated using photochemical cross-linking. T7 DNA homogeneously labeled with $^{3}H$ was partially degraded with E. coli exonuclease III to generate short, single stranded regions at both ends of the molecule. It was then repaired with E. coli DNA polymerase I and $\alpha$-$^{32}P$-labeled dNTP. This produced a T7 DNA molecule whose left end, which contains the three major promoters recognized by E. coli RNA polymerase was double labeled, with $^{32}P$ in the "sense" strand and $^{3}H$ in the "non-sense" strand. Both specific and non-specific binary RNA polymerase-T7 DNA complexes were exposed to UV radiation at 254 nm in order to induce stable linkages between enzyme and DNA. The cross-linked complexes were treated with nucleases to digest the free DNA and then subjected to SDS polyacrylamide gel electrophoresis. The gel was analyzed for the comigration of $^{3}H$ or $^{32}P$ radioactivity with the individual subunit bands. This allowed the identification of the DNA strand interacting with a particular subunit. The results indicated that under specific binding conditions, when binary complexes occur only at the major promoter sites, the $\sigma$ subunit discriminates between the two DNA strands, interacting almost exclusively with the non-sense strand. In contrast,no strand discrimination was observed under non-specific binding conditions when enzyme-DNA complexes form in all regions of the DNA. The strand specific interaction of $\sigma$ subunit at promoter sites suggests that $\sigma$ may act as an "unwinding" protein. This hypothesis is consistent with previous observations that $\sigma$ is required for formation of "open" promoter complexes and that the unwinding of superhelical DNA can be carried out by holoenzyme ($\alpha_2\beta\beta'\sigma$) but not by core enzyme ($\alpha_2\beta\beta'$). The strand specificity in the interaction of the $\beta$ and $\beta'$ subunits with DNA is currently being studied in our laboratory.

**T-PM-Po26** INTERACTION OF DNA WITH A PORPHYRIN LIGAND. James Howard*†, Ester Mark* and Robert Fiel, Department of Biophysics Research, Roswell Park Memorial Institute, Buffalo, New York, 14263.

The binding of meso-Tetra(4-N-methypyridyl)porphine perchlorate (4-MPyP) to DNA in aqueous solution was studied by U.V./visible spectroscopy, viscometry, thermal denaturation and circular dichroism (CD) spectroscopy. Porphyrin-DNA binding can be detected by the hypochromism of the 260 nm band for DNA and the porphyrin Soret band at 424 nm. A slight red-shift of the Soret band can also be detected. The relative viscosity of porphyrin bound DNA shows a maximum increase of approximately 11% over that of ligand-free DNA. Porphyrin bound DNA also exhibits an altered melting profile characterized by an increase in the Tm and a decrease in hyperchromism. CD measurements were made in the U.V. and visible regions. The positive DNA band at 279 nm was found to split into a doublet with smaller amplitude in the presence of 4-MPyP. The doublet is composed of a peak at 284 nm and a shoulder at 268 nm. The negative band at 248 nm for free DNA shows a slight shift to shorter wavelength and a reduced amplitude upon binding with 4-MPyP. The free porphyrin in solution shows no evidence of self-stacking and does not exhibit circular dichroism in either the U.V. or visible region; however, CD is induced when 4-MPyP is bound to DNA. A positive band occurs at approximately 427 nm and a negative band of somewhat less amplitude at 447 nm. The amplitude of the positive band increases with an increasing ratio of DNA/porphyrin. The negative band is ionic strength dependent and does not occur in 1 M NaCl. The evidence suggests at least two binding modes for this ligand, "intercalation" and "external binding".

†Supported by NIH ES-07057-01

**T-PM-Po27** ESR SPIN LABEL STUDIES OF MONONUCLEOSOME AND HISTONE PROTEIN CORE. D. C. F. Chan* and L. H. Piette, Cancer Center of Hawaii, University of Hawaii, 1997 East-West Road, Honolulu, Hawaii 96822

The spin label, N-(2,2,5,5-Tetramethyl-3-carbonyl-pyrrolidine-1-oxyl)-imidazole (IMDSL) has been used to study the accessibility and conformational state of tyrosines in both mononucleosomes and histone core particles extracted from chicken erythrocytes. IMDSL has been shown to be competitive with N-acetylimidazole for tyrosines in the histone core. About 40% of the tyrosines in the histone core can be labeled under nondenaturing conditions. This agrees with the Laser-Raman spectroscopy study by Olins et al. (Science, 197, 385, 1977), who showed that 60% of the tyrosines are hydrogen-bonded within the inner histones. The effect of urea on the conformational state of spin labeled tyrosines in both mononucleosome and in the histone core have been studied. Noncooperative and cooperative transitions are observed in both cases. Ionic effects on the spin labeled mononucleosome have been investigated. Several conformational transitions are observed in the range of 1 mM to 2 M NaCl. There is only a minor conformational change in the region of 1 mM to 100 mM NaCl. Three major transitions are found between 0.1 M to 0.6 M, 0.7 M to 1.5 M and 1.5 M to 2 M NaCl respectively. Circular dichroism for the spin-labeled mononucleosome has also been studied as a function of ionic strength. It was found that there is a decrease of $\alpha$-helix of the protein core observed at 225 nm in the region of 0.2 M to 0.6 M NaCl, however, the $\alpha$-helical content returns to its original value in the region of 1 M to 2 M NaCl. The ellipticity for DNA at 285 nm, however, increases gradually and slowly as the ionic strength is increased from 1 mM to 0.2 M NaCl. A sharp increase occurs at 0.5 M NaCl and reaches a maximum at about 1.5 M NaCl, it decreases again as the ionic strength is further increased. Our spin labeling and CD data provide complementary results for the effects of ionic strength on the monomer.

T-PM-Po28 CROSS-LINKING HISTONES IN RAT LIVER NUCLEI WITH A REVERSIBLE REAGENT. L. F. Levinger* (Intr. by J. Hermans), Department of Biochemistry 231H, University of North Carolina, Chapel Hill, N.C. 27514.

Cross-linked H1-H1 dimers include the heterotypic form (H1A-H1B) as well as the homotypic forms (H1A-H1A) and (H1B-H1B). This result rules out the possibility that H1 subspecies are entirely segregated from each other in liver nuclei. H1 cross-links to core histones are also observed, in addition to those formed between H1 subtypes.

A24, a form of H2A containing a covalently attached molecule of ubiquitin, has also been cross-linked to core histones, suggesting that it is a nucleosomal protein. An H2A-H2A dimer has been resolved from other histone dimers by first-dimension acid-urea, second-dimension discontinuous SDS gel electrophoresis with reversal of cross-links between dimensions. Detection of an H2A-H2A contact is consistent with results from other laboratories, including those showing histone-DNA cross-linking in nucleosome core particles.

T-PM-Po29 MICROCOCCAL NUCLEASE DIGESTS CHROMATIN IN NUCLEI AND IN SOLUTION WITH DIFFERENT CATALYTIC EFFICIENCIES. C. W. Carter, Jr. and L. F. Levinger*, Department of Biochemistry 231H, University of North Carolina, Chapel Hill, N.C. 27514.

Digestion of chromatin in nuclei, measured as the change in the concentration of monomer-length DNA with time, displays Michaelis-Menten kinetics. Redigestion of soluble chromatin prepared from nuclei by micrococcal nuclease treatment, however, is apparently first-order in enzyme and independent of chromatin concentration. This qualitative difference results from a true increase in the apparent second-order rate constant, $k_{cat}/K_m$, for liberation of monomer DNA: the apparent $K_m$ value for soluble chromatin is lower by three orders of magnitude than that for chromatin in nuclei, whereas $k_{cat}$ values differ by at most one order of magnitude.

Neither the integrity of the nuclear membrane nor the presence of histone H1 is essential for the dissociating kinetic behavior characteristic of chromatin in nuclei. Moreover, differences due to the buffers used for digestion and redigestion are minimal. Dissociating behavior is, however, correlated with the presence of higher-order chromatin superstructure.

Micrococcal nuclease added to soluble chromatin under non-digesting conditions at low ionic strength (I=0.002) co-sediments with chromatin in sucrose gradients. In 0.15M NaCl added nuclease no longer sediments with chromatin and redigestion kinetics become first-order in both enzyme and substrate with a greatly reduced value of $k_{cat}$.

Kinetic analysis of this type may afford an assay for native, higher-order structures in chromatin. Our results support the conclusion that micrococcal nuclease binds to soluble chromatin through additional interactions which do not occur in nuclei. Since these new interactions are abolished by moderate salt concentrations, they may be partly ionic in nature.

T-PM-Po30 FLUORESCENCE STUDIES OF INNER HISTONES. A. P. Butler*, and D. E. Olins, Univ. of Tenn.-Oak Ridge Grad. Sch. of Biomed. Sci., Biol. Div., Oak Ridge Natl. Lab., Oak Ridge, TN 37830.

The inner histone complex (equimolar amounts of H2, H2B, H3 and H4) was isolated from chicken RBC chromatin by 2 M NaCl extraction. The intrinsic tyrosine fluorescence of the histones and the fluorescence enhancement of a bound extrinsic fluorophore, 8-Anilino-1-naphthalene sulfonate (ANS) were examined as a function of solvent pH and ionic strength. Tyrosine fluorescence intensity increases at pH <5 (in 2 M NaCl), although studies with the collisional quencher KI indicate no increase in exposure of the Tyr residues. These alterations correlate with circular dichroism changes previously reported (Butler, et al., 1978, Biophys. J., 21, 66a), apparently reflecting subunit dissociation and a partial loss of α-helix due to the protonation of Asp and Glu. Tyr fluorescence intensity decreases between pH 8-10, due to formation of tyrosinate. ANS binds to inner histones in 2 M NaCl; binding is accompanied by a 50-55 nm blue shift and an increase in intensity of ANS fluorescence. This behavior is characteristic of ANS interaction with hydrophobic regions of proteins. The wavelength of maximum ANS fluorescence is blue-shifted an additional 8-10 nm at pH <5 (2 M NaCl), supporting the exposure of less polar residues as the inner histones dissociate. At pH 7.0 (NaCl <1 M) the binding of ANS to inner histones involves a large electrostatic component; at NaCl >1 M), other interactions predominate and the intensity of ANS fluorescence increases, possibly as a result of stabilization of higher oligomers (e.g. octamers).
[Research sponsored by the Div. of Biomed. & Environ. Research, U.S. Dept. of Energy under contract W-7504-eng-26 with the Union Carbide Corp. and NIH grant GM 19334 (DEO).]

**T-PM-Po31** CORE NUCLEOSOMES BY DIGESTION OF RECONSTRUCTED HISTONE-DNA COMPLEXES. Philip N. Bryan.* (Introd. by A. L. Olins), Univ. of Tenn.-Oak Ridge Grad. Sch. of Biomed. Sci., Biology Division, Oak Ridge National Laboratory, Oak Ridge, TN 37830.

Reconstructed complexes of the inner histones (H2A, H2B, H3, H4) and a variety of DNAs were digested with micrococcal nuclease to yield very homogeneous populations of core nucleosomes ($\nu_1$). Nucleosomes containing Micrococcus luteus DNA (72% G+C); Clostridium pyrfringens DNA (29% G+C); chicken DNA (43% G+C); or poly(dA-dT)·poly(dA-dT) have been examined by electron microscopy, circular dichroism (CD), thermal denaturation, hydrodynamics, and DNAse I digestion. DNAse I digestion of $\nu_1$(dA-dT) produces a ladder of DNA fragments differing in length by one base residue. $\nu_1$(dA-dT) contain 146 base pairs of DNA and exhibit an average DNA helix pitch of 10.4-10.5 bases per turn. CD spectra of all particles show a typically suppressed ellipticity at 260-280 nm and prominent α-helix signal at 222 nm. All particles show biphasic melting except $\nu_1$(dA-dT), which show three prominent melting transitions at ionic strengths $\leq$ 1 mM.
(Research supported jointly by the National Cancer Institute grant CA09104 and the Division of Biomedical and Environmental Research, U.S. Department of Energy under contract with the Union Carbide Corporation.)

**T-PM-Po32** HIGHER ORDER STRUCTURE IN CHROMATIN. J. B. Rattner[1] and B. A. Hamkalo[1,2], Department of Molecular Biology and Biochemistry[1] and Developmental and Cell Biology[2], University of California, Irvine, California 92717 U.S.A.

The elucidation of a particulate chromatin subunit, the nucleosome, as a ubiquitous component of eukaryotic chromatin has lead to the investigation of the manner in which these subunits are organized into higher order structures in both interphase and metaphase chromatin. We found that minimally disrupted higher order fibers can be visualized from mouse $L_{929}$ cells after gentle mechanical cell lysis with 0.5 mm glass beads in the presence of Joklik's suspension media. These continuous fibers uniformly measure 200-300A° in diameter and are composed of closely-apposed arrays of nucleosomes. At metaphase these fibers can be seen extending from the chromosome as a series of loops 1-5 μm in length. The presence of this higher order fiber in both interphase and metaphase preparations suggest that this fiber class is present within cells independent of the degree of chromatin condensation. Negatively stained preparations have allowed the identification of several distinct packing patterns within the higher order fiber. The variety of packing conformations and their variable distribution along the length of the higher order fiber suggest that although the diameter of the fiber is uniform, it is formed by folding the basic 100A° fiber non-uniformly.
(Research sponsored by NIH GM23241 and NSF PCM 78-08930)

**T-PM-Po33 ASYMMETRY OF INTRA-NUCLEAR FUNCTION DURING IMMUNE LYMPHOCYTE ACTIVATION.** John H. Frenster, Michael M. Papalian*, Marilyn A. Masek*, and Jeffrey A. Frenster*. Department of Medicine, Stanford University, Stanford, California 94305, and the Institute for Medical Research, Santa Clara Valley Medical Center, San Jose, California 95128.

The DNA helix must open in localized areas before the interior base-coded genetic information can be used for new RNA or DNA synthesis (Cancer Res. 36, 3394 (1976). Such DNA helix openings can be visualized, measured, and counted by a high-resolution electron microscopic technique (J. Natl. Cancer Inst. 59, 839 (1977) which was used to determine the location, size, and number of in-vivo DNA helix openings (Nature 248, 334 (1974) within 502 individual cells in the neoplastically-involved lymph nodes of untreated patients with Hodgkin's Disease (Natl. Cancer Inst. Monogr. 36, 239 (1973). The 437 normal lymphocytes were found to be of three cytoplasmic types, monosomal, transitional, and polysomal, reflecting progressive activation of the lymphocyte cytoplasm. Lymphocytes apposed to neoplastic Hodgkin and Reed-Sternberg cells were found to contain increased numbers of DNA helix openings, compared to non-apposed lymphocytes, with significant asymmetry of distribution of DNA helix openings into that half of the lymphocyte nucleus closest to the apposing neoplastic cell. Within the subset of apposed lymphocytes, the degree of asymmetry of intra-nuclear function increased progressively from monosomal lymphocytes through transitional lymphocytes to polysomal lymphocytes. This activation of immune lymphocytes in Hodgkin's Disease (Lancet 2, 167 (1974) may be mediated by the transfer of de-repressor immune RNA from the neoplastic cell to the proximal half of the nucleus of the immune T-lymphocyte (J. Natl. Cancer Inst. 60, 335 (1978)

Supported in part by Research Grants CA-10174 and CA-13524 from the National Cancer Institute, by Research Grant IC-45 from the American Cancer Society, and by a Research Scholar Award from the Leukemia Society.

**T-PM-Po34** THE PROXIMITY OF THE 3' TERMINI OF TWO TRNAS ON THE RIBOSOME. Barbara D. Wells[1] and Charles R. Cantor[2]. [1]Biophysics Department, Johns Hopkins University, Baltimore, MD and [2]Departments of Chemistry and Biological Sciences, Columbia University, New York, NY.

Yeast $tRNA^{phe}$ was periodate oxidized and labeled on the 3' end with either dansyl hydrazine or fluorescein thiosemicarbazide. The two fluorescent dyes were chosen as a good donor-acceptor pair for fluorescence energy transfer. The tRNAs were bound to poly U programmed E. coli ribosomal tight couples in 25mM magnesium at 10°C. The fluorescence properties of the dyes were used to determine the amount of tRNA bound. Energy transfer was observed as donor quench, then from knowledge of the amount of quench and the quantity bound the transfer distance was calculated to be 33 Å. Aminoacyl tRNA in the A site and tRNA in the P site should yield a distance between the 3' ends of about zero for peptidyl transfer. Clearly the fluorescently labeled tRNA we have used is not a good model for aminoacyl tRNA in the A site. However, it may be a good model for deacyl tRNA binding to the A site, a condition required for the stringent response. If this suggestion is correct, the displaced position of the 3' end of the tRNA in the A site may be the signal which promotes the binding of stringent factor to the ribosomes.

**T-PM-Po35** DIRECT OBSERVATION OF DISSOCIATION OF POLYRIBONUCLEOTIDE STRANDS: SCATTERING VS ABSORPTION IN THE UV. J. W. Preiss and P. C. Berry*, University of Delaware, Newark, Delaware, 19711.

Under certain conditions the turbidity of aqueous polyribonucleotide-globular protein mixtures is a sharply nonmonotonic function of polynucleotide concentration, possessing one maximum. This peak is more than an order of magnitude higher if components are mixed above the melting temperature of the polynucleotide (J. Chem. Phys. 65, 2913, 1976; Biophys. J. 13, 470, 1973). Such mixtures, containing only 5 µg of nucleic acid and 15 µg of protein per ml, are visibly turbid, and remain so after cooling to room temperature; protein and single polynucleotide strands are locked in very large, stable light-scattering centers of low density. The phenomenon makes possible quantitative and inexpensive detection of the dissociation of complementary or other multiple polynucleotide strands with visible light (qualitative with no optical device). Of course the light-scattering power increases inversely with some power of the wavelength (not the 4'th because of severe internal interference); in fact, at $\lambda$ = 259 nm (at which polyU and polyA have absorption maxima), the scattering coefficient is more than 5x the combined absorption coefficients for nucleic acid and protein components. Hence, multiply-scattered uv photons are absorbed outside the primary light beam and the probability of absorption in a given volume of fluid is greatly increased. If possible, demonstrations will be provided.

**T-PM-Po36** ANALYSIS OF GENOME INTEGRITY DURING EXPOSURE OF CULTURED MAMMALIAN CELLS TO CADMIUM CHLORIDE. C.E. Hildebrand and R.A. Walters, Cellular and Molecular Biology Group, Los Alamos Scientific Laboratory, The University of California, Los Alamos, New Mexico 87545 U.S.A.

To determine whether the toxic trace metal, cadmium (Cd), causes damage to DNA in mammalian cells, we have examined one indicator of DNA damage, the introduction of strand breaks and alkali labile lesions. Chinese hamster cells (line CHO) uniformly labeled with $^{14}C$-thymidine were exposed to $CdCl_2$ in suspension culture. Cellular DNA was analyzed by alkaline sucrose gradient sedimentation. DNA from unexposed cells sedimented in a single peak of $4.5 \times 10^8$ modal molecular weight (MW). Analysis of DNA from cells exposed to toxic $Cd^{++}$ levels (2 µM) for 24 h gave a bimodal DNA distribution (characteristic of nonrandom DNA breakage) having a peak of modal MW $8 \times 10^5$ and a high MW peak similar to the unexposed control profile. Since $Cd^{++}$ accumulates in cells during exposure, the question arises as to whether DNA breakage is also cumulative. To answer this question, DNA from cells exposed to 3 µM $CdCl_2$ for various intervals was analyzed for strand breaks. In the first 20 h of $Cd^{++}$ exposure, during which cells accumulate $Cd^{++}$ to the maximal level, no DNA breakdown was observed indicating that a simple relationship between strand breakage and cellular $Cd^{++}$ "dose" does not exist. After 20 h the amount of DNA sedimenting in the low MW mode increased with increasing time while there was no further intracellular $Cd^{++}$ accumulation. Comparison of the fraction DNA in the low MW mode with the fraction of non-viable cells (determined by the trypan blue exclusion assay) accumulating in the population with time showed a 1:1 relationship. These findings indicate that (1) DNA strand breakage is not a primary consequence of $Cd^{++}$ exposure and (2) the observed DNA breakdown is directly correlated with metabolic cell death. (This work was performed under the auspices of the U. S. Department of Energy.)

T-PM-Po37 DNA REPLICATION IN dna A TEMPERATURE SENSITIVE MUTANTS OF ESCHERICHIA COLI.
H. Eberle, N. Forrest* and J. Van Knapp*, University of Rochester School of Medicine and Dentistry, Rochester, New York 14642.

The dna A gene product has been previously demonstrated to be essential for the initiation of DNA replication of the Eschrichia coli chromosome. Work from other laboratories suggest that the dna A product acts early in the initiation process and it has been suggested that it may regulate the synthesis of a primer RNA postulated to be necessary for the initiation of DNA replication at the chromosomal origin.

We have examined the replication pattern of several temperature sensitive mutants with apparent defects in the initiation process. We have found that in temperature reversible dna A mutants it is possible to demonstrate prolonged DNA synthesis for up to 5 hrs. at nonpermissive temperatures after a certain growth regimen. The conditions which are prerequiste for the prolonged DNA synthesis at nonpermissive temperature (NPT) include: a prior period at nonpermissive temperature of 40-60 min, followed by return to the permissive temperature in the presence of chloramphemicol for at least 10 min. The rec A gene product also appears to be essential for the prolonged DNA synthesis at NPT in these dna A mutants. A characterization of the DNA synthesized for prolonged period at NPT suggests that the synthesis is semiconservative and is probably synthesis which commences at random sites on the chromosome as well as possible reinitiation events at the origin. The implications of these results to the regulation of DNA replication will be discussed.

This paper is based on work performed under contract with the U.S. Department of Energy at the University of Rochester, Department of Radiation Biology and Biophysics and has been assigned UR-3490-1493.

**T-PM-Po38** KINETICS OF SELF-ASSOCIATION FOR GLUTAMATE DEHYDROGENASE
H.R. Halvorson, E.B. Ford Institute for Medical Research, Detroit 48202.

Relaxation kinetics of glutamate dehydrogenase self-association have been determined using small (ca. 8 atm) repetitive (1000-2000 times) pressure perturbation and monitoring the resulting changes in Rayleigh scattering at an angle of 90°. The change in weight-average molecular weight is small (ca. 0.1%), assuring the validity of the approximations used in relaxation kinetics. There is but a single concentration-dependent relaxation and the concentration dependence of the relaxation times demonstrates the validity of the random indefinite self-association model proposed by Thusius (J. Mol. Biol. 92:413). The activation volume (+350 ml/mol) provides clues to the molecular mechanism involved. A rapid shift in scattered light intensity is attributed to preferential interaction between phosphate anion and the protein, proceeding with a positive volume change (2-5 ml/mol phosphate). The way in which the kinetic parameters vary with changes in pH and ionic strength permits further insights into the nature of the self-association interaction.

Supported by NIH GM 23302

**T-PM-Po39** EFFECTS OF NUCLEOSIDE TRIPHOSPHATES ON THE SUBUNIT INTERACTION ENERGIES OF E. COLI ASPARTATE TRANSCARBAMYLASE. N.M. Allewell, A. Zaug*, and G.E. Hofmann*, Wesleyan University Middletown, CT. 06457

Changes in the subunit interaction energies of E. coli aspartate transcarbamylase produced by the binding of the allosteric inhibitor, CTP, and the allosteric activator, ATP, have been evaluated over the pH range 7-9. Values for $\Delta G_{binding}$, $\Delta H_{binding}$, and $\Delta S_{binding}$ to both the native enzyme and regulatory subunit were derived from thermal titration curves obtained by microcalorimetry. The changes in the subunit interaction energies produced by the binding of the effector are equal to the differences between the corresponding quantities for the native enzyme and regulatory subunit. While binding of either nucleoside triphosphate causes $\Delta H_{interaction}$ to become more negative by several kcal/mole, the change in $\Delta G_{interaction}$ is minimal, because of compensating changes in $\Delta S_{interaction}$. The dependence of $\Delta H_{binding}$ on $\Delta H_{ionization}$ of the buffer indicates that differences between the native enzyme and regulatory subunit in the proton uptake effects which accompany binding account for a substantial portion of the change in $\Delta H_{interaction}$.

**T-PM-Po40** MECHANISM OF TOBACCO MOSAIC VIRUS ASSEMBLY: INCORPORATION OF 4S AND 20S PROTEIN AGGREGATES AT pH 7.0 AND 20°c. S. J. Shire, J. J. Steckert* and T. M. Schuster, Biological Sciences Group, University of Connecticut, Storrs, CT 06268.

A method is described for the preparation of Tobacco Mosaic Virus protein consisting of greater than 97%, by weight, 20S disk aggregates at 20°c in 0.1 M ionic strength orthophosphate buffer at pH 7.03. The method takes advantage of the relatively slow rate of depolymerization of 20S to 4S protein which under these conditions makes it possible to neglect the 20S to 4S interconversion during reconstitution. This 20S disk preparation can be used with various concentrations of 4S protein to study the relative efficiency of incorporation of 4S versus the pre-assembled 20S disk protein during the post-nucleation phase of the reaction. After mixing an excess of the protein components with TMV RNA the resulting protein and reconstituted virus sedimentation coefficients and concentrations are obtained directly by analytical ultracentrifugation. Electron microscopy is used to investigate the quality of the reconstituted virus. The data strongly suggest that both the 4S and 20S protein components participate in the elongation phase during assembly, but that the 4S component incorporates preferentially.

Supported by NIH Grants AI-11573 and AI-05266.

**T-PM-Po41** GRAPHICAL ANALYSIS OF NON-IDEAL MONOMER N-MER AND ISODESMIC INDEFINITE SELF-ASSOCIATING SYSTEMS. W.F. Stafford III, Rosenstiel Center, Brandeis Univ., Waltham, MA 02154.

Concentration dependent behavior of the apparent weight average molecular weight, $M_{w,app}$, for a non-ideal monomer N-mer or isodesmic indefinite self-associating system can be described by a monomer molecular weight, an equilibrium constant and an activity coefficient. For an ideal monomer N-mer self-associating system, one can generate a set of standard curves by plotting $\log(M_{w,app}/M_1)$ *vs.* $\frac{1}{N-1}\log(K_N c^{N-1})$ for various stoichiometries as parametric functions of the weight fraction, $\alpha$, of polymer (*cf.* Yphantis and Roark, 1972). By direct comparison to experimental data plotted on the same scale as $\log(M_{w,app})$ *vs.* $\log(c)$, one can obtain, in principle, the stoichiometry, monomer molecular weight and equilibrium constant by superposition of the plots. In addition, for non-ideal systems for which the logarithm of the activity coefficient can be represented as a linear function of c, one can generate for each stoichiometry a series of standard curves by introducing a single dimensionless parameter defined as $\beta=BM_1/K_N^{(N-1)}$ (where B is the colligative second virial coefficient, $M_1$ is the monomer molecular weight and $K_N$ the monomer N-mer association constant). From these curves one can obtain the second virial coefficient as well as the other parameters. What is notable about this approach to the analysis of non-ideal systems is that, for any given value of $\alpha$, deviations from ideality are shown to be dependent only on $\beta$. Furthermore, for systems which exhibit a maximum in the plot of $M_{w,app}$ *vs.* c, one can obtain both $K_N$ and $BM_1$ simply from a knowledge of $(M_{w,app}/M_1)_{max}$ and $c_{max}$ if the stoichiometry is also known. For example, it can be shown for a monomer-dimer system that: $(M_{w,app}/M_1)_{max}=(1+\alpha_{max})^3/(1+3\alpha_{max})$; $K_2=\alpha_{max}/(1-\alpha_{max})^2 c_{max}$; $\beta=0.5[(1-\alpha_{max})/(1+\alpha_{max})]^3$; $BM_1=\beta K_2$. Similar relationships for other stoichiometries and other molecular weight averages for both monomer N-mer and isodesmic indefinite self-associating systems will be presented. Supported by NHLBI grant # HL 21488.

**T-PM-Po42** ACID-INDUCED CONFORMATIONAL CHANGES IN HUMAN CHORIONIC GONADOTROPIN (HCG) AND THE MECHANISM OF SUBUNIT DISSOCIATION. H. Forastieri and K.C. Ingham, American Red Cross Blood Services, Plasma Fractions Laboratory, Bethesda, Md. 20014.

HCG is comprised of two nonidentical subunits held together by noncovalent bonds. Dissociation of the subunits in acid or in urea is strongly influenced by temperature. At 4°C, the intact hormone undergoes a conformational transition in acid which is characterized by: (1) a reversible increase in the polarization, P, of tyrosyl fluorescence from 0.19 at pH 7 to 0.22 at pH 3 with a midpoint at pH 5, (2) a slight decrease in the elution volume on Sephadex G-100 at pH 3 relative to pH 7, (3) a decrease in $S_{20,W}$ from 3.22 at pH 7 to 2.92 at pH 3, and (4) a small positive near UV difference spectrum ($\Delta\varepsilon \simeq 2\%$). These observations are compatible with an acid-expanded form of the hormone in which one or more tyrosines are less exposed to the solvent. The increased P at pH 3 is stable at temperatures as high as 7°C but decreases with time at higher temperatures. At 25° or 30°, P reaches an apparent plateau value within approximately 30 minutes which depends on the temperature, and which can be reversed by subsequent slow cooling. No detectable dissociation into subunits accompanies this decrease in P. Prolonged incubation for several hours at these temperatures will result in further decreases in P and dissociation into subunits. At 37°C, P decreases continuously with concurrent dissociation into subunits, but first order kinetics are not observed. These results suggest the occurrence of at least two conformationally distinct forms of HCG which are sequentially encountered prior to subunit dissociation in acid.

**T-PM-Po43** INTERPRETATION OF NON-LINEAR VAN'T HOFF AND ARRHENIUS PLOTS. E. D. Sprague,* C. Larrabee,* and H. B. Halsall (Intr. by E. Franke), Department of Chemistry, University of Cincinnati, Cincinnati, OH 45221.

It has been suggested that, in general, non-linear van't Hoff and Arrhenius plots for many processes involving proteins may be the result of a nonzero $\Delta C_p$ or $\Delta C_p^{\ddagger}$ for the process (H. J. Hinz, et al., Biochemistry, 10, 1347 (1971)). This may not always be the case, however, and it is important that a careful analysis be made of the experimental data to determine the correct form of the van't Hoff or Arrhenius plot. Using non-linear least squares techniques, it is possible to determine whether the data in a given case are better explained in terms of (1) nonzero heat capacity changes, or (2) a temperature-dependent equilibrium between two forms of the protein. We have examined, therefore, both kinetic and equilibrium data for systems involving the binding of steroids to serum proteins. The data of Basset, et al. (BBRC, 79, 380 (1977)) for the binding of cortisol to human corticosteroid binding globulin (CBG) fit best when model (2) is chosen. These results are compared with analyses of the binding of progesterone to CBG, progesterone binding globulin, and orosomucoid.

**T-PM-Po44** A NEW AND SIMPLIFIED CALCULATION OF THE INTRINSIC ENTROPY OF A PROTEIN SUBUNIT. Harold P. Erickson, Anatomy Department, Duke University Medical Center, Durham, NC 27710

The intrinsic entropy due to the translational and rotational freedom of a protein subunit is an important consideration in protein interactions and assembly. For polymerization to occur the bond energy, attributable to hydrophobic interactions at the subunit interfaces, must be sufficient to compensate for the loss of entropy as the subunit is immobilized (1, 2). A very simple calculation of this intrinsic entropy may be obtained on the basis of the following assumption: rotation and translation of the immobilized subunit are restricted, but only to a level of about 1 Å. Thermal vibration and movement of this magnitude are observed for individual atoms in protein crystals, and this is a reasonable estimate for the vibrational movement of surface atoms and the center of mass of the subunits in a protein polymer. The rotational entropy loss may then be given by $\Delta S_R = R \ln \alpha^3$, where $\alpha = 1/(\text{circumference})(1)$. For a 20,000 MW globular protein $\alpha = .009$ and $\Delta S_R = -28$ e.u. The translational entropy loss may be estimated as that involved in compressing the subunits from a hypothetical standard state of 1 M to a concentration where the centers of subunits are 1 Å apart (1667 M). Thus, $\Delta S_T = -R \ln(1667) = -15$ e.u.

The total loss of intrinsic entropy upon polymerization of a protein subunit is therefore 43 e.u., which corresponds to a free energy of 13 kcal/mol. This is about half the value obtained by quantum mechanical calculation with no correction for internal vibration (2), but it still represents a considerable energetic barrier to polymerization. Experimental data do not rule out the higher values, but are generally consistent with a total intrinsic entropy change of only -10 e.u. The value of -43 e.u. derived here may still be considerably higher than actually applies in protein association. Refs.: (1) Steinberg and Scheraga, J. Biol. Chem. 238: 172 (1963); (2) Chothia and Janin, Nature 256: 705 (1975).

**T-PM-Po45** INTERACTION OF AFLATOXINS WITH HUMAN LIVER IN VIVO AND IN VITRO. C. Kirk* and D. Yourtee, Cancer Research Center, Columbia, Mo. 65205.

Postmitochondrial fractions of human liver have been used to evaluate the ability of this tissue to bind the potent hepatocarcinogenic aflatoxins and to convert sequestered toxins to oxidized or reduced metabolites. As a measure of the in vivo interaction microsomal liver from 22 Missouri cancer patients was exhaustively extracted with chloroform and the extracts were evaluated using thin layer chromatography and scanning fluorometry techniques to determine the presence of aflatoxins $B_1$,$G_1$,$B_2$,$G_2$ and any metabolites of these that might have been formed in vivo. One of the specimens was found to contain aflatoxin $B_1$ at approximately 500 ng/g wet liver tissue. Incubation of this specimen with an NADPH generating system and the native aflatoxin produced traces of metabolite which, however, was in insufficient quantity for identification. In alternate experiments with the same population of liver samples, the in vitro metabolism of aflatoxin $B_1$ by human hepatic microsomes produced a number of metabolites that varied among individuals but was usually on the order of three to five metabolites per individual. There were high percentages of bound aflatoxin and the most common and quantitativly important metabolite among organosoluble metabolites was aflatoxin $Q_1$. This aflatoxin metabolite was produced by all age groups and in both sexes over a variety of liver histological and historical influences for the subjects providing the specimens. These findings support that human liver has a proclivity for aflatoxins and their metabolism. Although the critical interactions with tissue macromolecules might not be the same , sequestering of aflatoxin in liver microsomes and multiple metabolism has been observed in experimental animals susceptible to hepatomas from aflatoxins. Results for a larger population of human tissues will be discussed.

**T-PM-Po46** A PHYSICAL DESCRIPTION AND QUALITATIVE EXPLANATION OF DROPLET SEDIMENTATION. H. B. Halsall, Department of Chemistry, University of Cincinnati and C. J. Remenyik*, Engineering Science, University of Tennessee.

The resolution between fractions which have been separated by zone or zonal centrifugation may be reduced by a behavior of the initial sample overlay called droplet sedimentation. This phenomenon is the consequence of a fluid mechanical instability which develops under certain circumstances and may make separations entirely impossible. To gain a further insight into the initiation and propagation of the instability, direct visual observations were made under stationary conditions. Very simple geometric configurations and dynamic conditions were used to observe the formation of filaments and droplets from buoyant layers containing dense macromolecules. The development of the droplets into small vortex rings, and their motions were followed. In the simplest case, the initial degradation of a single drop of sample liquid, containing macromolecules, spread on the supporting primary liquid is into an annular filament developing at the periphery of the drop. This is the result of diffusional processes occurring at the liquid-liquid interface between the sample layer and the primary liquid, combined with the fact that the edge of the spreading drop has been in contact with the primary liquid longer than more central regions. After filament formation, normal liquid perturbations distort the shape of the filament, and may bend small portions upward or downward. Portions bent downward ultimately develop into droplets as a result of shear stresses and pressures in and around the villi.

**T-PM-Po47** LASER-INDUCED REACTIONS OF PYRIDOXAL SCHIFF BASES. J.W. Ledbetter, H.W. Askins*, and R.S. Hartman*, Department of Biochemistry, Medical University of South Carolina, Charleston, S.C. 29403.

In a model system for pyridoxal mediated enzyme catalysis of transamination a key intermediate has been produced and detected by pulsed lasers. Pyridoxal catalysis is thought to generate a p-quinoid intermediate which facilitates the aldimine ⇄ ketimine reaction. With the 3371 Å emission of the nitrogen laser this p-quinoid intermediate was produced by the excitation of the Schiff bases formed between pyridoxal and both aliphatic and aromatic aminoacid esters in methanol. Detection by a simultaneously pumped dye laser demonstrated that the intermediate was produced within the 10 ns uv pulse. Production of the intermediate was made possible by reacting the 3-hydroxyl group with $Al^{3+}$ at a low temperature. This partial chelation prevented the formation of an otherwise preferentially formed o-quinoid structure and allowed the formation of the p-quinoid structure. In addition, uv excitation of this p-quinoid intermediate, generated by the laser or not and from either direction of the above equilibrium, apparently produced the chelated aldimine. These results and those of some kinetic studies will be presented.

**T-PM-Po48** THE OXYGEN-18 KINETIC ISOTOPE EFFECT OF CHYMOTRYPSIN-CATALYZED ETHANOLYSIS. Michael H. Klapper and Chih-Lueh A. Wang*, Dept. of Chemistry, The Ohio State University, Columbus, Ohio 43210 and Lan K. Wong*, Dept. of Pharmacology, The Ohio State University, Columbus, Ohio 43210.

The α-chymotrypsin catalyzed alcoholysis of p-nitrophenyl (5-n-propyl)-2-furoate has been studied with $^{18}O$-labelled ethanol. The ethyl ester product was monitored as a function of time using a combined gas chromatography-mass spectrometry technique allowing comparison of the $^{18}O$ enrichment in the product relative to that in the ethanol. A large apparent $^{18}O$ kinetic isotope effect was observed at all tested conditions. The apparent kinetic isotope effect, which is normal near the beginning of the reaction, becomes inverse as the reaction proceeds. The changeover is qualitatively consistent with the postulate of an intermediate between furoyl chymotrypsin and the ethyl ester product.

**T-PM-Po49** NMR STUDIES OF THE INTERACTION OF CHROMIUM NUCLEOTIDES WITH CREATINE KINASE. Raj K. Gupta and Jeffrey L. Benovic* (Intr. by C.H. Fung) The Institute for Cancer Research, Philadelphia, PA 19111

$Cr^{3+}$-nucleotides replace $Mg^{2+}$-nucleotides at the active site of creatine kinase (Schimerlik and Cleland, J. Biol. Chem. 248, 8418). We have studied the paramagnetic effects of enzyme-bound CrATP and CrADP on the nuclear relaxation rates of the $^{31}P$ and $^{1}H$ nuclei of P-creatine. Although CrADP exerts a large paramagnetic effect on the nuclear relaxation rates of the $^{31}P$ nucleus of P-creatine ($1/T_{1M} = 675 \pm 120$), no significant paramagnetic effects ($1/T_{1M} \leq 15$) of CrATP on the $^{31}P$ and $^{1}H$ nuclei of P-creatine were detectable, arguing against simultaneous binding of CrATP and P-creatine at the active site of the enzyme. The inability of CrATP and P-creatine to bind simultaneously to creatine kinase indicates some spatial overlap of the γ-phosphoryl group of ATP with the phosphoryl group of P-creatine on the enzyme. From the magnitude of the paramagnetic effect of CrADP on the $^{31}P$ nucleus of P-creatine, a $Cr^{3+}$ to $^{31}P$ distance of $6 \pm 0.5$ Å is calculated. The simultaneous binding of CrADP and P-creatine and the $Cr^{3+} - {}^{31}P$ distance indicate the absence of a direct coordination of the nucleotide-bound metal by the transferred phosphoryl group of P-creatine on creatine kinase but support molecular contact between the phosphorus of P-creatine and the terminal β-oxygen of ADP, suggesting an $S_N2$ mechanism for the creatine kinase reaction. (Supported by NIH grants AM-19454, AM-13351 and USPHS RCDA AM-00231).

**T-PM-Po50** KINETICS OF PARACOCCUS NITRITE REDUCTASE. M. Robinson* and R. Timkovich, Ill. Inst. Tech., Chicago, Ill., 60616.

The integrated rate law for the reaction between donor cytochromes c and Paracoccus denitrificans cytochrome oxidase: nitrite reductase has been determined for either molecular oxygen or nitrite as terminal acceptor:

$$S = S_0 \exp\left[-U_1 t - \frac{U_2(S-S_0)}{1+U_3(S-S_0)}\right]$$

where S is the donor ferrocytochrome c concentration, t is time, and $S_0$ the initial donor concentration. The parameter $U_1$ is proportional to total enzyme concentration and inversely proportional to total (ferro plus ferri) cytochrome c concentration. $U_2$ and $U_3$ are independent of ferricytochrome concentration, but inversely proportional to ferrocytochrome concentration. Rates are independent of $O_2$ or $NO_2^-$ at concentrations greater than 50 μM of either. The implications are that the kinetic mechanism of this bacterial cytochrome oxidase is distinct from mechanisms proposed for mitochondrial oxidases. Product inhibition by ferricytochrome c is a possible scheme, but the enzyme then must bind the ferri and ferro forms of cytochrome c with different strengths.

**T-PM-Po51 ABSTRACT WITHDRAWN**

**T-PM-Po52** NITROGEN LIGAND ENDOR FROM COPPER IN L-ALANINE SINGLE CRYSTAL. R. Calvo, S.B. Oseroff and H.C. Abache (Intr. by C. Caputo), I.V.I.C., Caracas, Venezuela.

The ENDOR spectra of a nitrogen ligand of copper in single crystals of L-alanine have been measured as a function of angle at X-band and 4K. Our data allow us to obtain the magnetic huperfine and electric quadrupole tensors. The principal values are: $A_x$ = 27240 KHz, $A_y$ = 27600 KHz and $A_z$ = 41610 KHz and $Q_{x'}$ = 130 KHz, $Q_{y'}$ = 1490 KHz and $Q_{z'}$ = - 1620 KHz. A pseudo-nuclear spin-spin interaction between nitrogen and copper have been detected and explained. The principal values and orientation of the hyperfine coupling tensors measured by ENDOR are discussed together with the gyromagnetic tensor, and the hyperfine coupling of copper, measured by EPR in the same sample, in terms of the structure of the copper-L-alanine system. Supported in part by CONICIT, Venezuela.

**T-PM-Po53** $^{13}C$ and $^{113}Cd$ NMR of Metallothionein
J.D. Otvos* and I.M. Armitage, Yale University, New Haven, CT. 06510

Metallothionein is a small (MW6800), cysteine-rich metal binding protein found in the kidney and liver of a wide variety of animal species. The structural basis for its remarkable metal binding capacity (about 7 g-atoms metal/mole, usually zinc and/or cadmium) has been investigated by natural abundance $^{13}C$ NMR as well as by direct observation of the metal nucleus itself using $^{113}Cd$ NMR. At 67.9 MHZ the $^{13}C$ NMR spectra of rabbit liver metallothionein I and II exhibit numerous resolved resonances in the carbonyl and aliphatic regions, many of which can be assigned on the basis of their variation as a function of pH, metal ion content, and $^{1}H$ decoupling. $^{113}Cd$ NMR spectra of metallothionein I and II have also been obtained both at natural abundance and using enriched $^{113}Cd$ protein isolated from rabbits injected with $^{113}CdCl_2$. Multiple $^{113}Cd$ resonances are observed >600 ppm downfield from $CdClO_4$. These results will be discussed in terms of possible models for the metallothionein metal binding sites. (Supported by Grants ES01674 and AM 18778 from the NIH).

**T-PM-Po54** CARBON-13 NMR STUDIES OF THE STRUCTURE OF THE IRON-BLEOMYCIN COMPLEX. Rai K. Gupta, James A. Ferretti and William J. Caspary. Inst. Cancer Res., Phila., PA 19111; NIH, Bethesda, MD 20014, and NCI, NIH, Baltimore, MD 21211

Bleomycin $A_2$, an antitumor antibiotic, has one iron binding site as revealed by the iron-titrations of bleomycin monitored optically at 460 nm for $Fe^{2+}$ ($\Delta\varepsilon_{mM}^{460}$ = 0.225) and at 430 nm for $Fe^{3+}$ ($\Delta\varepsilon_{mM}^{430}$ = 2.0). The bleomycin-iron complex is believed to cause single strand breaks in DNA. Other metal ions, such as $Cu^{2+}$ and $Zn^{2+}$, inhibit this reaction. The bleomycin-$Fe^{2+}$ complex produces superoxide and hydroxyl radicals which may cause DNA strand breaks. We have shown that bleomycin acts like a ferrous oxidase in its reaction with oxygen to produce these reduced oxygen species. To further probe the structure of the iron-bleomycin complex, we studied the paramagnetic effects of the ferric iron on the longitudinal nuclear relaxation rates ($1/T_1$) of the aliphatic carbon atoms in the molecule. The addition of 0.7 mM $Fe^{3+}$ to a 51 mM solution of bleomycin enhances the $1/T_1$ of only four aliphatic carbon atoms in the molecule (C2, C3, C5 and C6 according to the numbering system in Biochem. 17, 4090). No other aliphatic carbon atoms were affected. From the magnitude of the paramagnetic effects of $Fe^{3+}$ on the $^{13}C$ relaxation rates, we obtain distances of 4.6, 5.3, 5.3 and 4.6 Å from the metal to the C2, C3, C5 and C6 carbon atoms, respectively. These results are consistent with the coordination of the α-amino group of the terminal diaminopropionic acid residue and the pyrimidine ring but do not implicate any other parts of the bleomycin molecule in binding to iron. Using $Mn^{2+}$ as a paramagnetic probe, our EPR studies reveal that the binding of various metal ions to bleomycin is mutually exclusive and that the metal-bleomycin interaction is strongly pH-dependent. The metal ion-inhibition of bleomycin action appears to result from displacement of iron from the iron-bleomycin complex by inactive metals. (RKG is supported by NIH grant AM19454 and RCDA AM00231).

**T-PM-Po55** METAL-BINDING STUDIES WITH BACITRACIN A, A PEPTIDE ANTIBIOTIC. D. Scogin,* H. Mosberg,* and R. B. Gennis, Department of Chemistry, University of Illinois, Urbana, 61801 and D. Storm,* Pharmacology Department, University of Washington, Seattle, Washington.

Bacitracin A is a membrane-active dodecapeptide antibiotic produced by strains of *B. licheniformis*. The primary structure has been previously determined. Bacitracin A is bacteriocidal by virtue of its ability to form a ternary complex with a divalent metal cation and bactoprenyl pyrophosphate, thus preventing the dephosphorylation of the lipid carrier and blocking cell wall biosynthesis. Storm and Strominger (J. Biol. Chem. 248, 3940 (1973)) demonstrated that bacitracin, in the presence of a metal ion, will form a strong complex with farnesyl pyrophosphate, a synthetic analog of bactoprenyl pyrophosphate. Our eventual aim is to study this complex as a model for protein-lipid interactions. Efforts so far have been to define the nature of the bacitracin-metal binary complex in solution. Complex formation has been monitored using (1) U. V. absorption spectroscopy, (2) proton release measurements, and (3) $^{1}H$ NMR. We have conclusively demonstrated 1:1 binding stoichiometry. The perturbation caused by the metal on the NMR of the bacitracin protons, and the pH dependence of the metal-bacitracin dissociation constant, have led to a proposal as to the metal coordination sites on bacitracin. The proposal has the metal ion coordinated to the imidazole of the histidine, to the glutamate, and to the thiazoline ring. Evidence indicates that the N-terminal α-amino group and the aspartate are not directly involved in the binding. Deprotonation of the N-terminal amino group within the metal-bacitracin complex results in precipitation of the complex.

**T-PM-Po56** CALCIUM AND MAGNESIUM ION BINDING TO BOVINE PROTHROMBIN FRAGMENT 1. K.A. Koehler, R.G. Hiskey*, P. Robertson, Jr.*, M.E. Scott*, and H.C. Marsh*, University of North Carolina, Chapel Hill, NC 27514.

The concentration and pH dependence of calcium and magnesium ion binding to bovine prothrombin fragment 1 have been investigated by observation of: (1) metal ion-induced fluorescence quenching, (2) metal ion-dependent changes in secondary structure (as reported by protein ellipticity changes at 232 nm, 220 nm, and 208 nm), and (3) $^{25}Mg^{2+}$ and $^{43}Ca^{2+}$ nuclear magnetic resonance linewidths in the presence of fragment 1. From these data a model is developed which clarifies the relationship between calcium ion and magnesium ion binding to fragment 1. Such a model is important for the understanding of phospholipid binding by fragment 1 in the presence of calcium ions.

**T-PM-Po57** CHEMICAL SHIFT TENSORS FOR $^{15}N$ IN HISTIDINE.
G. S. Harbison, J. Herzfeld and R. G. Griffin*, Biophysical Laboratory, Harvard Medical School, Boston, MA 02115 and Francis Bitter National Magnet Laboratory, Massachusetts Institute of Technology, Cambridge, MA 02139.

The chemical shift tensors for $^{15}N$ in L-histidine HCl were determined by three orthogonal rotations of single crystals in a 68 kG field. The chemical shift of the amino nitrogen is 24.8 ppm, relative to crystalline $(NH_4)_2SO_4$, with an anisotropy of less than 12 ppm. For the two imidazole nitrogens, the most shielded tensor elements are, as expected, essentially orthogonal to the ring plane and nearly equal in magnitude. Tentative assignment of the tensors was made possible by the fact that one principal axis of each tensor was found to lie approximately in the direction of one of the N-H bonds. For N-1 of the imidazole ring, the principal values of the chemical shift are $\sigma_{11}$=37.6 ppm, $\sigma_{22}$=197.0 ppm and $\sigma_{33}$=260.9 ppm. For N-3, the eigenvalues are $\sigma_{11}$=33.6 ppm, $\sigma_{22}$=169.6 ppm and $\sigma_{33}$=250.6 ppm. The calculated isotropic chemical shifts for the two ring nitrogens in the crystal differ by 12 ppm. By way of comparison, the published solution values of the imidazole chemical shifts, at low pH, differ by only 2.1 ppm. It has been reported that solution values of the imidazole chemical shifts are markedly pH dependent. In order to examine the spatial details of the change in chemical shift on deprotonation, we are currently undertaking a single crystal study of Bis-(L-histidinato) cadmium dihydrate, an unprotonated complex of histidine. (Supported by grants GM 23316 and GM 23403 from NIH, and C-670 from NSF.)

**T-PM-Po58** FLUORESCENT LABELING OF THE CARBOHYDRATE MOIETY OF $\alpha_1$-ACIDGLYCOPROTEIN (AGP) AND HUMAN CHORIONIC GONADOTROPIN (HCG). Kenneth C. Ingham and Shelesa A. Brew, American Red Cross Blood Services, Plasma Fractions Laboratory, Bethesda, Maryland 20014.

The dansyl fluorophore was covalently attached to sialic acid residues of AGP and the α subunit of HCG using periodate oxidation at pH 5 followed by reaction with dansyl hydrazine and subsequent reduction with $NaBH_4$. Labeling ratios of 2.5 and 1.5 moles/mole of protein were estimated for AGP and HCG-α respectively. Treatment of dansyl-AGP with neuraminidase at pH 5.1 and 37°C caused a linear decrease in the polarization (P) of dansyl fluorescence from 0.17 to 0.12 after 1 hour. Exclusion chromatography of the product revealed that ~50% of the dansyl fluorescence appeared near the salt volume, presumably conjugated to the liberated sialic acid residues. A labeling ratio of 1.3 was estimated for the partially desialated dansyl-AGP. The P for dansyl-HCG-α (50 μM) increased from 0.038 to 0.045 immediately after addition of its complementary β subunit (100 μM) at 37° and pH 7. This was followed by a further increase to 0.063 with $t_{1/2} \simeq 20$ min. Exclusion chromatography of the product indicated that all of the dansyl-HCG-α eluted in the position of the intact hormone which has $M_r$ close to that of AGP. The much higher P for dansyl-AGP relative to dansyl-HCG-α and its recombinant with the β subunit suggests that the dansyl group has less rotational freedom in AGP, perhaps reflecting a more rigid carbohydrate structure relative to that in HCG-α.

**T-PM-Po59** WATER-RELAXATION TIMES OF NORMAL, PRENEOPLASTIC, AND MALIGNANT PRIMARY CELL CULTURES OF MOUSE MAMMARY GLAND. P.T. Beall, B.B. Asch,* D.C. Chang, D. Medina,* and C.F. Hazlewood, Depts. of Pediatrics, Physiology, and Cell Biology,* Baylor College of Med., Houston, TX 77030.

Distinction between normal, preneoplastic, and malignant tissues, by nuclear magnetic resonance (NMR) relaxation times, $T_1$ and $T_2$, of water protons has been reported. Part of these differences may be due to the mixture of fat cells, connective tissues, blood and lymph volumes, necrotic regions, and increased hydration in tumors. To determine if any portion of these NMR differences is due to intracellular changes, we explored the phenomenon in primary cell cultures of mouse mammary glands, in which we had already shown significant NMR differences in the whole tissues. Tissues were aseptically removed, minced, and incubated in collagenase to disassociate the cells. Cells were plated into Dulbecco's MEM with 13% fetal bovine serum and supplements. D-valine was substituted for L-valine to discourage the growth of fibroblasts. After 4-5 days in primary culture the cells were harvested for NMR determinations and centrifuged at $\sim$ 1200 g for 40 min. $T_1$ was measured by a $180^\circ$-$\tau$-$90^\circ$ pulse sequence and $T_2$ by a Carr-Purcell spin echo method on a Bruker SXP-NMR spectrometer at 30 MHz and 25°C. The $T_1$s of normal, preneoplastic alveolar nodule (HAN-$D_2$) and malignant adenocarcinoma ($D_2$) cells were 916 ± 24 ms, 1029 ± 24 ms ($p < .005$) and 1155 ± 42 ms ($p < .001$) respectively. The $T_2$ values were 158 ± 6 ms, 187 ± 7 ($p < .01$), and 206 ± 8 ($p < .001$). Percent water content of cell pellets was 90.8 ± 0.4 for normal, 90.0 ± 0.5 ($p > .7$) for preneoplastic, and 91.4 ± 0.2 ($p > .3$) for malignant cells. A significant portion of the difference in water proton relaxation times, appears to be cellular in origin and independent of hydration. (Supported by GM-20154, CA-11944, CA-21624, Welch Q-390, and ONR N00014-76-C-0100 and 78-C-0068.

**T-PM-Po60** LOW ANGLE X-RAY DIFFRACTION OF DERMATOSPARACTIC LAMB SKIN. K. Cassidy*, B.Brodsky, E. Eikenberry*, CMDNJ-Rutgers Medical School, Piscataway, New Jersey 08854.

Dermatosparaxis is a heritable disorder of collagen in which the amino terminal precursor peptide is not cleaved due to lack of a specific enzyme activity. Comparison of the x-ray diffraction of normal and dermatosparactic lamb skins may indicate how the peptide extension affects the structure of the collagen in the diseased state. Wet normal lamb skin showed more than 20 orders of the 670Å meridional spacings reflecting the axial staggering of the molecules. The dermatosparactic lamb skin when wet gave almost no discernable meridional reflections. Two separate treatments of the dermatosparactic skin brought up the meridional reflections: a) drying the specimen and b) reduction of the disulfide bonds. Electron microscopy showed a 640Å axial repeat in the dermatosparactic skin which is inconsistent with the wet x-ray data. However, x-ray diffraction of dried dermatosparactic skin gave intense meridional reflections which suggests that drying caused the structure to become more ordered than it was in the wet state. The intrachain disulfide bonds in the amino terminal peptide extension are the only disulfide bonds in the molecule, and these bonds are necessary to maintain the native three dimensional conformation of the peptide. The improvement in orientation seen in the x-ray diffraction pattern after reduction suggests that the steric hindrance due to the native conformation of the amino terminal peptide extension causes the lack of axial order seen in the untreated dermatosparactic lamb skin.

**T-PM-Po61** REVERSIBLE UNFOLDING OF DIHYDROFOLATE REDUCTASE. C. R. Matthews, W. Stratton,* N. Touchette,* and D. Baccanari,* Penn State Univ., University Park, PA 16802.

The urea and guanidine hydrochloride (Gdn-HCl) induced unfolding of dihydrofolate reductase (DHFR) from E. coli (strain RT 500) in a solution containing 10 mM Tris-Cl, pH 7.2, 0.1 mM $K_2$EDTA, and 1 mM 2-mercaptoethanol was monitored by UV difference spectroscopy at 285 and 292 nm. The difference spectrum at these two wavelengths reflects changes in the solvent exposure of tyrosine and tryptophan residues, respectively. Analysis of the unfolding curves as a function of denaturant concentration and the coincidence of the unfolding transitions at the two wavelengths support a two-state model for this process. The free energy of stabilization of the native form calculated from these data is in the range of 4 to 6 kcal/mole for both urea and Gdn-HCl. Similar to other proteins lacking disulfide bonds, DHFR is unfolded by relatively low concentrations of denaturant; denaturant concentration at the midpoint of urea and Gdn-HCl induced unfolding is 2.9 and 1.5 M, respectively. Modification of a single cysteine with p-azidophenylacyl bromide and subsequent photolysis apparently can result in the introduction of a covalent crosslink in DHFR. When the photolyzed protein is unfolded by urea, two unfolding transitions are apparent. The first corresponds to that observed for unmodified DHFR and the second, at higher denaturant concentration, to a more stable species of the protein. The increased stability is presumably due to the formation of a covalent crosslink between the initially labeled cysteine and residues in close proximity. The existence of two approximately equal populations of protein, crosslinked and noncrosslinked, can be attributed to the reaction of the nitrene either with the protein or with solvent or other components in solution. Investigations on the location of the crosslink(s) are in progress. This work was supported by PHS grant GM24570.

**T-PM-Po62** ANALYSIS OF PROTEIN FOLDING KINETICS IN TERMS OF NUCLEATION, GROWTH, AND MERGE OF HYDROPHOBIC DROPLETS. Minoru I. Kanehisa* and Tian Yow Tsong, Department of Physiological Chemistry, The Johns Hopkins University School of Medicine, Baltimore, Maryland 21205.

The kinetics of the cluster model of protein folding (Kanehisa & Tsong, Biophys. J. 21 (1978) 38a; J. Mol. Biol. 124 (1978) 177-194) are further investigated by a new representation of the cluster distribution; namely, the probability of finding the polypeptide chain of length N with k ordered regions (clusters) and m ordered residues (residues in the cluster) is represented on a contour map (k,m). The time evolution of this probability distribution, which is treated as a stochastic process, is analysed after a sudden change of the external condition. Typical folding and unfolding processes are consistent with the following schemes.

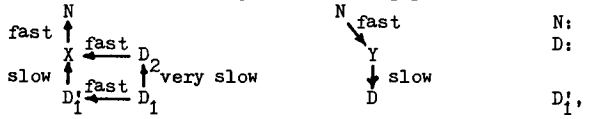


N: Native population
D: Denatured population where $D_1$ and $D_2$ are fractions of D
$D_1'$, X, Y: Kinetic intermediates

The equilibrium and kinetic properties of the cluster model are characterized by the surface free energy of the cluster, which is highly dependent on the external condition. The separation of the fast and slow steps in the above schemes, as well as their transition dependence, is analysed by considering possible changes in this surface free energy.

The cluster model favors the following pictures. Protein folding starts with the nucleation and growth of hydrophobic droplets, followed by the merge of these droplets into larger ones. Conversely, protein unfolding is determined by the growth and merge of locally unfolded regions (defects). Both droplets and defects are dynamic quantities and are responsible for the fluctuation of protein structure. (Supported by NSF Grant PCM 75-08690.)

**T-PM-Po63** A TAXONOMY FOR PROTEIN STRUCTURES
J. Richardson, Duke Univ., Durham, N.C. 27710.

A system is presented for classifying the overall three-dimensional folding patterns for all the distinctly different domains found in the known protein structures. Schematic drawings are shown for all of these domains, arranged according to the classification system: in four major categories and subgroups within those.

I. Antiparallel α
  a. Up&down helix bundles (e.g., hemerythrin)
  b. Greek key helix bundles (e.g., myoglobin)
II. Parallel α/β
  a. Singly-wound parallel barrels (e.g., triose-P isomerase)
  b. Doubly-wound parallel sheets (e.g., lactate dehydrogenase$_A$)
III. Antiparallel β
  a. Up&down β barrels (e.g., rubredoxin)
  b. Greek key β barrels (e.g., immunoglobulin domains)
  c. Antiparallel sheets (e.g., concanavalin A)
IV. Small disulfide-rich or metal-rich proteins
  a. Toxin-agglutinin fold (e.g., erabutoxin)

**T-PM-Po64** VIBRATIONAL SPECTRA OF BETA-TURNS IN POLYPEPTIDES AND PROTEINS. Jagdeesh Bandekar* and S. Krimm, University of Michigan, Ann Arbor, MI 48109.

Beta-turns have come to be recognized as significant components of the structures of globular proteins. It is important, therefore, to know the characteristic vibrational frequencies associated with β-turns of different types. We have calculated the normal vibration frequencies for a type I β-turn of $CH_3$-CO-$(Ala)_4$-NH-$CH_3$ and a type II β-turn of $CH_3$-CO-$(Ala)_2$-Gly-Ala-NH-$CH_3$. In these calculations we used the force field that was refined in our laboratory for β-sheet and α-helical structures. A calculation was also done for $CH_3$-O-CO-Gly-$(Ala)_2$-Gly-O-$CH_3$, which is an appropriate model for two tetrapeptides for which infrared and Raman data are available. The agreement between observed and computed frequencies for these molecules is good. The most important result of the calculations is the prediction of amide I bands near 1690 $cm^{-1}$, a region heretofore associated only with the antiparallel-chain pleated sheet structure. We also find that a band near 1665 $cm^{-1}$ is characteristic of type II turns. A survey of protein structures shows that deviations in dihedral angles of β-turns from the ideal values are frequent and often large. We have calculated the effects of such deviations on the amide frequencies, and these results will be discussed.

This research was supported by NSF grants PCM76-83047 and CHE78-00753.

**T-PM-Po65** COMPLEXITY GOVERNS THE DIRECTION OF DETERMINISTIC MOLECULAR PROCESSES. Brian K. Davis, Long Island Research Institute, Health Sciences Center, SUNY-Stony Brook, N.Y. 11794.

The transmission of complexity during DNA replication has been investigated to clarify the significance of this molecular attribute in a deterministic process. In this study, complexity was equated with the amount of randomness within ordered molecular structures, and it was measured by the entropy of a posteriori probabilities for discrete (monomer sequences) and continuous (torsion angle sequences) structural parameters in polynucleotides, proteins, and ligand molecules. The measure employed is a function of both the total number and variety of structural elements (monomers, angles, bonds); conversely, exp(average complexity) specifies the variety of elements. A theoretical analysis revealed that complexity decreases during transmission from a monomer sequence in DNA to one in a protein. It was also found that sequence complexity limits the attainable complexity in the folding pattern of a polypeptide and that a protein cannot interact with a ligand moiety of higher complexity. Furthermore, the analysis indicated that in any deterministic molecular process a cause possesses more complexity than its effects. This outcome is broadly consistent with Curie's symmetry principle. Results from an analysis of an extensive set of experimental data corroborate these findings. It is evident, therefore, that complexity governs the direction of order-order molecular transformations. In fact, its role in deterministic processes is comparable with that of thermodynamic entropy, or the equivalent quantity, information, in order-disorder phenomena. Two biological implications are (i) replication of DNA in a stepwise, repetitive manner by a polymerase seems to be a necessary consequence of structural constraints imposed by complexity, and (ii) during evolution, increases in complexity had to involve chance. This latter requirement apparently applied also to development of the first replicating system, regardless of the conditions on Earth at the time life began. (Supported by NIH grant HD12998)

**T-PM-Po66** THEORY OF THE SPECIFIC KERR CONSTANT OF RIGID, CHARGED, DIPOLAR, ELLIPSOIDAL MACROMOLECULES IN CONDUCTING SOLUTION IN THE ABSENCE OF CONDENSED COUNTERIONS. S. Krause, B. Zvilichovsky*, and M. E. Galvin*, Department of Chemistry, Rensselaer Polytechnic Institute, Troy, N. Y. 12181.

In the previous theoretical treatment of the Kerr Constant of rigid, dipolar, conducting ellipsoidal macromolecules (O'Konski and Krause, 1970, J. Phys. Chem., 3243), a surface conductivity was postulated directly on the surface of each macromolecule. In the case of charged macromolecules, this surface conductivity was assumed to be caused by movement of condensed counterions on the macromolecules. In the present work, the case of a macromolecule with a low charge to surface area ratio has been examined at very low ionic strength. Under these circumstances, one expects essentially no condensed counterions. In this case, it has therefore been assumed that the average counterion is at the Debye characteristic distance from the surface of each charged macromolecule and contributes to surface conductivity at that distance, with no additional surface conductivity on the true surface of the macromolecule. These considerations change the calculated interaction energy of the macromolecule with an externally applied electric field. Changes occur in both the internal field components of the applied field and in the reaction field of the macromolecular dipole. The new interaction energy is used to calculate the orientation distribution function of the macromolecules in dilute solution and this distribution function can, in principle, be used to calculate the steady state electric linear or circular dichroism, electric light scattering, anisotropy of conductivity, etc., as well as the specific Kerr Constant which will be shown here. A comparison with the predictions of the O'Konski-Krause theory will be presented.

**T-PM-Po67** RAMAN SPECTROSCOPY OF INTACT PRIMATE LENSES WHICH HAVE CATARACTS INDUCED BY ULTRAVIOLET RADIATION. K. L. Schepler and D. Thomas*, USAF School of Aerospace Medicine, Brooks AFB, TX 78235.

The eyes of mature rhesus monkeys have been exposed to ultraviolet radiation (337 nm) from a nitrogen laser. The laser operated in a pulsed mode with 4 mJ per pulse at 10 pulses per second. Exposure durations ranged between 2 and 10 seconds. Immediately following the exposures, opacities were observed in the anterior region of the lens. After removal from the eyes, exposed lenses were deposited in an opti-cell containing a balanced salt solution and Raman spectra were recorded. Spectral results of normal lens areas indicate a rich fingerprint region (400-1800 $cm^{-1}$) and considerable water content as revealed in the 3200-3600 $cm^{-1}$ region. Positions of the amide I and III vibrations indicate a β-pleated sheet structure. Raman spectra of cataractous areas show changes in the 3200-3600 $cm^{-1}$ region. More subtle changes are observable in the fingerprint region.

The animals used in this study were procured, maintained, and used in accordance with the Animal Welfare Act of 1970 and the "Guide for the Care and Use of Laboratory Animals" prepared by the Institute of Laboratory Animal Resources-National Research Council.

T-PM-Po68 SEPARATION OF MACROMOLECULES BY ULTRAFILTRATION THROUGH MICROPOROUS MEMBRANES.
Thomas F. Busby and Kenneth C. Ingham, American Red Cross Blood Services, Plasma Fractions Laboratory, Bethesda, Maryland 20014.

Fractionation of different sized polymers by ultrafiltration is complicated by the accumulation of rejected species on the membrane surface which decreases flux and alters the effective sieving properties. Thus, a small polymer, which in pure solution is unrejected by the membrane, may be substantially rejected when larger polymers are present. In this study, mixtures of albumin and poly(ethylene glycol), PEG-4000, were used to elucidate some of the factors which govern separation efficiency on the Amicon TCF-10 thin-channel device using a PM-30 membrane, an applied pressure of 20 psi, and a sample circulation rate of 210 ml/min. When PEG (50 mg/ml) was diafiltered in the absence of albumin, its concentration decreased exponentially with the number of volumes exchanged; a 10-fold reduction was obtained after 2.3 volumes indicating no rejection. In the presence of 50 mg/ml albumin, which did not penetrate the membrane, the flux decreased ~ 5-fold, and PEG was partially rejected such that 4.4 volumes were required to effect a 10-fold reduction in concentration. When albumin was removed and the system flushed with water, the flux was not fully restored and the rejection of PEG in the absence of albumin was similar to that with 5% albumin present. When the membrane was treated with trypsin, the original properties were recovered. Diafiltration of PEG in the presence of as little as 0.001% albumin was sufficient to cause deterioration of membrane performance as subsequently measured in the absence of protein. These results suggest that dynamic concentration polarization is not as important as irreversible protein adsorption in determining the efficiency of macromolecular separations. Preliminary experiments suggest that efficiency may be improved by manipulation of solution conditions such as pH and ionic strength which influence protein adsorption to surfaces.

**T-PM-Po69** IMMUNOFLUORESCENCE STAINING OF HONEYBEE Z-DISC PROTEINS. Judith D. Saide* and Solveig G. Ericson* (Intro. by W.C. Ullrick) Boston University School of Medicine, Boston, MA 02118.

Isolated Z-discs are prepared by treating honeybee myofibrils with 0.5% lactic acid. Sodium dodecyl sulfate gel electrophoresis of purified Z-disc preparations resolves at least four proteins with subunit molecular weights of 87,000, 158,000, 175,000 and 360,000 daltons (Saide and Ullrick, J. Mol. Biol. 87:671, 1974). Antibodies to each of these polypeptides have been produced by injecting rabbits with homogenized gel slices containing the individual components. By indirect immunofluorescence it is found that antibodies to the 87,000, 158,000 and 175,000 dalton polypeptides bind specifically to the Z-bands of honeybee myofibrils. Antibodies to the 360,000 dalton protein, however, are localized along the sides of the Z-band, not at its center. With this antibody, fluorescence is limited to narrow bands at the edges of the Z-lines of shortened fibrils, but extends from the Z-lines to the A-bands in stretched fibrils. These results suggest that the 360,000 dalton protein is associated with the connecting filaments which join thick filaments to the Z-band in insect indirect flight muscle. The study confirms that the 87,000, 158,000, and 175,000 dalton proteins, identified in gels of isolated Z-discs, in fact originate from the intact Z-band. (Supported by grant-in-aid #13-513-767 from the Massachusetts Affiliate of the American Heart Association, B.U.S.M. Biomedical Research Support Grant #PHS 05380, N.I.H. grant #PHS 1 R01 HL22985, and a Muscular Dystrophy Association grant to J.D.S. This work was done during the tenure of an Established Investigatorship of the American Heart Association (J.D.S.).

**T-PM-Po70** COMPARISON OF ADULT, EMBRYONIC AND DYSTROPHIC CHICKEN MUSCLE MYOSINS BY SDS ELECTROPHORESIS AND PEPTIDE MAPPING. Julie Ivory Rushbrook* and Alfred Stracher, SUNY-Downstate Med. Center, Brooklyn, N.Y. 11203.

Chicken myosin from adult fast white fibers, both normal and dystrophic, adult slow red fibers, adult muscle containing both fast white and fast red fibers, and embryonic pectoralis muscle were compared by direct electrophoresis in Laemmli SDS slab gels and by the Cleveland peptide mapping technique. Direct electrophoresis in 5% gels revealed that the myosin heavy chain present in adult slow red fibers migrated more slowly than the heavy chains from the other sources, which have similar migration rates. Electrophoresis of the light chains in 15% gels produced the patterns expected for myosins from adult fast white fibers, adult slow red fibers, and embryonic pectoralis muscle. Light chain-1 from dystrophic fast white fibers migrated more slowly than its counterpart in normal tissue. Two light chains, in addition to those from myosin of fast white fibers, were present in myosin from adult muscle containing fast white and fast red fibers. Comparison of myosin heavy chains by the Cleveland peptide mapping procedure showed large differences between adult myosins from fast white and slow red fibers, as expected from other studies. The map of myosin from adult dystrophic fast white fibers was very similar to that of its normal counterpart but slight differences were noted. The peptide maps of myosin heavy chains from embryonic pectoralis muscle resembled the pattern from myosin of adult fast white fibers but showed definite differences. The pattern obtained from myosin of the mixed fast white-fast red fibers contained bands present in the maps of embryonic pectoralis myosin and adult fast white fiber myosin. The data show that the myosin heavy chain from embryonic pectoralis muscle differs from that of the adult muscle (fast white fiber type) and may be similar to that in adult fast red fibers. (Supported by M.D.A. Inc.)

**T-PM-Po71 FURTHER STUDIES ON THE PROTEOLYSIS OF LOBSTER MYOSIN.**
**+R.F. Siemankowski, H. Manuel*, C. Richard Zobel. +Dept. of Nutrition & Food Science, Univ. of Arizona, Tucson, Ariz., 85721 & Dept. of Biophysical Sciences, State Univ. of N.Y., Buffalo, N.Y., 14214.**

**Previous results have shown that proteolysis of lobster abdominal muscle myosin with $\alpha$-chymotrypsin, papain or trypsin results in the production of a number of ethanol resistant rod-like fragments that are insoluble at neutral pH and low ionic strength. The fragments produced by limited tryptic digestion have been fractionated into three polydisperse populations which have been characterized by SDS-gel electrophoresis, equilibrium ultracentrifugation and electron microscopy. Double-dimensional analysis shows that in addition to the molecular weight heterogeniety evident in the rod fractions by SDS-gel electrophoresis there is marked charge heterogeniety as well. The soluble supernatant from limited tryptic digestion contains 40% (w/w) of the original myosin in the form of small peptides plus two fractions (approximately 25% of the original myosin) that are precipitable at 50% and 65% $(NH_4)_2SO_4$. The fraction that precipitates at 65% $(NH_4)_2SO_4$ saturation has a specific ATPase activity of 1.7$\mu$M Pi/min/mg.($K^+$-EDTA), a mol. wt. of ca. 80,000 Mr and is apparently analogous to subfragment-1 from vertebrate skeletal myosin. Of the two light chains, LC2 is resistant to fragmentation by trypsin and $\alpha$-chymotrypsin but the 20,000 Mr LC1 is enzymatically sensitive. Both light chain species appear to contain several charged variants when run by double-dimensional electrophoresis. In the presence of $Ca^{++}$ LC1 is not fragmented by $\alpha$-chymotrypsin.**

T-PM-Po72 $CA^{2+}$ BINDING PROPERTIES OF UNPHOSPHORYLATED AND PHOSPHORYLATED CARDIAC AND SKELETAL MYOSINS. Michael J. Holroyde*, James D. Potter and R. John Solaro ( Intr. by M. Behbehani ) University of Cincinnati, College of Medicine, Cincinnati, OH 45267.

Porcine left ventricular cardiac myosin and rabbit white skeletal myosin were phosphorylated by rabbit skeletal muscle myosin light chain kinase. $Ca^{2+}$ binding measurements were carried out on unphosphorylated and phosphorylated cardiac and skeletal myosin using equilibrium djalysis with EGTA to regulate the $Ca^{2+}$ concentration in the presence or absence of $Mg^{2+}$. Results obtained with this technique show no significant effect of phosphorylation on the $Ca^{2+}$ binding characteristics of these two myosins. In contrast to these results on native myosins, phosphorylation has been reported to exert a considerable effect on the $Ca^{2+}$ binding properties of isolated skeletal myosin light chains ( Alexis and Gratzer, Biochemistry, 17, 2319-2325, 1978). Our results show that both cardiac and skeletal myosin bind approximately two moles of $Ca^{2+}$ with similar affinities of $3 \times 10^7 M^{-1}$. In the presence of 0.3 mM $Mg^{2+}$ the myosins bind $Ca^{2+}$ with a reduced affinity of $3\text{-}4 \times 10^5$ $M^{-1}$. Assuming competition between $Ca^{2+}$ and $Mg^{2+}$ for the binding sites on myosin, the changes in $Ca^{2+}$ binding may be accounted for by a myosin $Mg^{2+}$ affinity of $2.5\text{-}3 \times 10^5$ $M^{-1}$. According to these results about 0.7 moles $Ca^{2+}$ per mole myosin will be bound at $10^{-5}$ M free $Ca^{2+}$ assuming the in vivo free $Mg^{2+}$ concentration is 2.5 mM as reported by Dawson et al. ( Nature, 274, 861-866, 1978 ). However, in view of its slow kinetics (Bagshaw, Biochemistry, 16, 59-67, 1977), the physiological signivicance of myosin $Ca^{2+}$ binding remains unclear. ( Supported by grants from the American Heart Association and National Institutes of Health, NHLBI )

T-PM-Po73TIME COURSE OF CHANGES IN PROTEIN DEGRADATION, CATHEPSIN B ACTIVITY AND WEIGHT OF SKELETAL MUSCLES WITHIN IMMOBILIZED HIND LIMBS OF RATS. M.J. Seider and F.W. Booth*, Department of Physiology, University of Texas Medical School, Houston, Texas 77030.

The hind limbs of rats were immobilized with plaster of paris for varying durations. The release of tyrosine from *in vitro* soleus and gastrocnemius muscle in the presence of cycloheximide was used as an index of protein degradation. In 60-70 gram rats, a significant ($P < 0.05$) increase in the release of tyrosine from the soleus was observed after one day of immobilization. However, no significant weight loss in the soleus was observed until the third day of immobilization. Cathepsin B activity did not significantly change during the first 3 days of immobilization. When the hind limbs of 250-300 gram adult rats were immobilized, significant increases in activities of cathepsin B and D preceded any significant loss of muscle weight. Activities of cathepsin B and D in gastrocnemius of adult rats were significantly elevated by the second day of immobilization although wet weight did not significantly decline until day 3 of immobilization. In the soleus of adult rats, cathepsin B and D activities significantly increased by days 2 and 3 of immobilization, respectively, but the wet weight did not significantly change during this period. These data suggest that increases in the activity of cathepsin B in atrophying skeletal muscle within immobilized limbs of young rats do not always precede the increase in protein degradation or the net loss of muscle mass. However, in adult animals, increases in cathepsin activity appear to precede changes in muscle mass. (Supported by NIH Grant AM-19393 and NASA).

T-PM-Po74 EFFECTS OF $Ca^{++}$ AND EGTA ON SKELETAL MYOSIN AGGREGATION WITH AND WITHOUT C-PROTEIN. Mark V. Bloom* and Jane F. Koretz, Rensselaer Polytechnic Institute, Troy, NY 12181

Differences in hydrodynamic behavior of isolated natural thick filaments and synthetic myosin filaments in the presence and absence of $Ca^{++}$ have been attributed to movement of the myosin crossbridges away from the filament backbone (Morimoto and Harrington, J. Mol. Biol., 1974), although no difference in head mobility is observable by time-resolved fluorescence anisotropy decay (Mendelson and Cheung, Sci., 1976). Our electron microscopy results indicate that filaments prepared from column-purified myosin in the presence of either 0.1mM $Ca^{++}$ or 0.1mM EGTA, or in the absence of control of either species at 0.1M KCl, 10mM Imidazole, pH7.0, demonstrate no differences in length or diameter distribution, and the myosin heads are close to the backbone. Filaments prepared under the same conditions, but with C-protein added before dialysis in a molar ratio of 1 to 3.3 myosin molecules, also demonstrate heads close to the backbone, suggesting that hydrodynamic differences must arise from other causes. The presence of EGTA (or the lack of $Ca^{++}$) in the myosin - C-protein filaments, however, affects aggregation in that the resultant aggregates are different in both appearance and structure from filaments prepared under all other conditions cited. (Supported by NIH Grant NS-14377).

**T-PM-Po75** BINDING OF ADDED C-PROTEIN TO MYOFIBRILS AS OBSERVED BY FLUORESCENCE MICROSCOPY. C. Moos, Biochem. Dept., SUNY, Stony Brook, NY 11794.

C-protein is a component of the thick filaments of skeletal muscle. In vitro at low ionic strength, it binds not only to myosin but also to F-actin (Moos, et al, J.Mol.Biol, in press). Fluorescence microscopy of intact myofibrils with added fluorescein-labeled C-protein, and also with added native C-protein plus fluorescein-labeled anti-C-protein, has now been used to investigate two questions: (1) Can C-protein interact with native thin filaments? (2) Can extra C-protein bind to the thick filaments, particularly in regions where C-protein is not normally present? The answer to both questions appears to be "yes". (1) In 0.1 M KCl, added C-protein binds strongly to the I-band of myofibrils, in a much larger amount than is initially present in the A-band. A gap can be seen at the Z-line. The binding to the I-band is inhibited in the presence of subfragment-1, as was observed for C-protein binding to pure F-actin. However, unlike the latter, the binding to the I-band is Ca-dependent: labeling of the I-band is intense in 0.1 mM $Ca^{++}$ but virtually absent in 1 mM EGTA. Thus C-protein-actin interaction can occur in native thin filaments and may be regulated by the Ca-troponin system. (2) When I-band labeling is suppressed by S-1 or EGTA, binding of added C-protein to the A-band becomes observable. The entire A-band is labeled, with the central portion near the M-line sometimes appearing brighter. Thus the absence of C-protein from the central and peripheral parts of the A-band in vivo is apparently not due to an inability of the myosin assembly in these regions to bind C-protein. (This work was done while the author was a Visiting Scientist at the MRC Cell Biophysics Unit, Univ. of London King's College, England. It was also supported in part by NSF Grants PCM 73-06715 and 77-26785 and by the Muscular Dystrophy Association.)

**T-PM-Po76** OBSERVATION OF THE MYOSIN SUBFRAGMENT-1·ADP COMPLEX BY $^{31}P$ AND $^{19}F$ NUCLEAR MAGNETIC RESONANCE SPECTROSCOPY. J.W. Shriver, J.H. Baldo and B.D. Sykes, M.R.C. Group on Protein Structure and Function, Department of Biochemistry, University of Alberta, Edmonton, Canada, T6G 2H7.

The myosin subfragment-1·ADP complex (M*ADP) has been observed using $^{31}P$ NMR. Interference due to exchange with the M*ADP·$P_i$ ternary complex has been eliminated by enzymatic removal of orthophosphate. Even in highly purified preparations orthophosphate is continuously produced in concentrated myosin samples by contaminating adenylate kinase coupled with the myosin ATPase activity. Phosphate is removed by the nucleoside phosphorylase catalyzed phosphorolysis of nicotinamide riboside (Rowen & Kornberg, J. Biol. Chem. 193, 497 (1951))

$$NR + P_i \rightleftharpoons \text{Nicotinamide} + R\text{-}1\text{-}PO_4 + H^+$$

The bound β-phosphorous of ADP in the M*ADP complex gives three narrow lines in the $^{31}P$ NMR spectrum. This indicates three forms of bound ADP in approximately equal concentrations which are in slow exchange. The relationship of these forms to light chain content is being investigated.

The myosin subfragment-1·2F-ADP complex has been observed by $^{19}F$ NMR. Determination of the chemical shift tensor element magnitudes for 2F-ADP has made it possible to identify chemical shift anisotropy relaxation as the dominating contribution to the linewidth of the bound 2F-ADP resonance. The results indicate that the 2F-ADP is rigidly bound to a non-flexible region of the subfragment-1 molecule.

**T-PM-Po77** PHOTOLYSIS IN THE STUDY OF ATPases. L.G.Herbette, J.H.Kaplan[1], T.Kihara[2], J.A.McCray[1] and D.R.Trentham, Department of Biochemistry and Biophysics, University of Pennsylvania, Philadelphia, PA 19104. [1]Department of Physiology and Biophysics, University of Iowa, Iowa City, Iowa 52242. [2]Department of Physics and Atmospheric Science, Drexel University, Philadelphia, PA 19104.

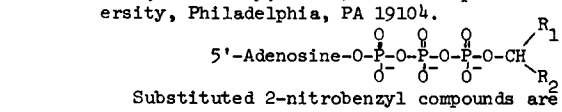


I. $R_1 = CH_3-$, $R_2$ = 2-nitrophenyl-

II. $R_1, R_2$ = 2-nitro-4,5-dimethoxyphenyl

Substituted 2-nitrobenzyl compounds are photolysable so that compounds such as I afford the possibility of introducing ATP into biological organelles in a way that does not result in ATP degradation when ATPases are present. Kaplan et al. (Biochemistry,17,1929-35,1978) have synthesized I and shown its value for studying the $Na^+/K^+$ ATPase. An alternative route to I is described in which the nitrobenzyl phosphate is first prepared as the barium salt and then condensed with ADP using carbonyl di-imidazole to activate the nucleotide.

Experiments following the incubation of I with rabbit skeletal myosin subfragment 1 and isolated sarcoplasmic reticulum $Ca^{2+}$ ATPase as closed membrane vesicles show that as with the $Na^+/K^+$ ATPase there is only weak if any binding of I to the proteins so that photolysed I or freshly introduced ATP can immediately react with these enzyme systems. I has a relatively broad action spectrum centered near 330 nm. The susceptibility of I to rapid photolysis with 30 ns pulses using a 347 nm frequency-doubled ruby laser or using shuttered continuous irradiation is described. II may have advantages over I in that a pair of diastereoisomers is not formed during its synthesis (Patchornik et al.,J.Am.Chem.Soc.92,6333-5,1970) and the parent alcohol ($\varepsilon$ $1.07 \times 10^4$ $M^{-1}cm^{-1}$ at $\lambda$max 343 nm) absorbs light much more effectively than I in the 347 nm region enhancing the potential of II for rapid reaction studies.

**T-PM-Po78** INACTIVATION OF MYOSIN SUBFRAGMENT ONE ATPASE BY INCORPORATION OF CO(III) BY ELECTRON TRANSFER BETWEEN CO(III)(PHEN)$_2$ AND ENZYME-BOUND COBALT II(PHEN) COMPLEXES. James A. Wells, Moshe M. Werber* and Ralph G. Yount, Washington State University, Biochemistry/Biophysics Program and Department of Chemistry, Pullman, WA 99164

Reinvestigation of the previously reported inactivation of myosin ATPase by Co(III)ATP(phen) $O_2^-$ (Biochemistry 13, 2683 (1974)) has shown that the inactivation can best be attributed to labeling of myosin by electron transfer from enzyme-bound Co(II) to a Co(III)(phen)$_2$ complex rather than by substitution of an enzyme ligand for $O_2^-$. Addition of Mg ADP (0.1 mM) accelerates the rate of inactivation of myosin subfragment one (SF-1) ATPase 10-fold at pH 8.0, 1 mM Co(III)(phen)$_2$CO$_3$, 0.1 mM $CoCl_2$, 0.1 mM 1,10-phen, 0.01 mM SF-1, 0.1 M KCl, 0°C. Inactivation is pseudo 1st order for 3 half lives with $t_{1/2}$ ≈ 1 min. Studies with $^{57}$Co indicate up to 0.5 cobalts are rapidly incorporated into a non-critical site while a second critical cobalt binds to two thiols believed to be at or near the active site. Enzyme bound cobalts are believed to be exchange inert Co(III) since they cannot be removed by dialysis for 3 days against 5 mM EDTA or 1,10-phen but are completely removed by brief treatment with $NaBH_4$, DTE, or Fe(II) EDTA. Treatment with Fe(II) EDTA regenerates 95-100% of the ATPase activity indicating no extraneous modification of the protein has occurred. Inactivations of SF-1 with Co(II)(phen), ATP and $H_2O_2$ cannot be reversed by Fe(II) EDTA. Use of various Co(II)/Co(III) couples represents a potential mild general method for incorporating Co(III) into metal binding sites of proteins. Supported by grants from MDA, AHA of Washington and NIH (AM-05195).

**T-PM-Po79**DISSOCIATION AND REASSOCIATION OF THE MYOSIN OLIGOMER: ATPase ACTIVITY, $Ca^{2+}$ BINDING, AND DEGREE OF LIGHT CHAIN RELEASE. J. Wikman-Coffelt, San Francisco Univ., San Francisco, Ca. 94143.

Myosin appears to go through a conformational change with an increase in temperature resulting in a partial dissociation of the light chains. Both alkali and DTNB light chains of rabbit skeletal muscle myosin dissociate from the heavy chains during a brief incubation in the $K^+$/EDTA kinetic system. There is an increased release of both classes of light chains with increments of temperature from 25° to 37°, and with increments of pH from 6.5 to 9.0. Dissociation of alkali light chains is time-dependent whereas release of DTNB light chains is concentration-dependent. The substrate, ATP, protects the active site of myosin during treatment; there is a 20% dissociation of both alkali light chains and a 75% release of the DTNB light chain with no corresponding decrease in $K^+$ or $Ca^{2+}$ stimulated ATPase activities, when treatment is at 37° for 10 min in the presence of 5 mM ATP, and at a neutral pH. Frog skeletal muscle myosin light chains dissociate in the presence of EDTA at 4°. For both frog and rabbit skeletal muscle myosin, divalent cations help prevent dissociation of the DTNB but not release of the alkali light chains. Reassociation of rabbit skeletal muscle myosin with light-chain-deficient myosin is dependent on time, temperature, and the presence of divalent cations. Loss in myosin ATPase activity during light chain dissociation is not regained with reassociation of the myosin oligomer. With dissociation of DTNB light chains there is a corresponding decrease in number of $Ca^{2+}$ binding sites, however, the released light chains have a decreased affinity for $Ca^{2+}$ in the Tris.maleate, pH 6.5 $Ca^{2+}$-binding system: The released light chains do not show the cooperativity in calcium binding which is present with native myosin. After reassociation of light chains with light-chain-deficient myosin the high affinity $Ca^{2+}$ binding sites are regained.

**T-PM-Po80** INTERACTIONS OF CONTRACTILE PROTEINS WITH CIBACRON BLUE F3GA. A.P. Toste and R. Cooke, Cardiovascular Research Institute, Univ. of California, Medical Center, San Francisco, CA 94143. (Intr. by Joseph Leung)

The dye, Cibacron Blue F3GA, inhibits the ATPase activities of skeletal myosin and myosin subfragment-1 (S-1), as well as tension generation by rabbit psoas fibers. Myosin's and S1's actin-activated and $Ca^{2+}$ ATPases are completely inhibited, with half-maximal inhibition occurring at 15 μM dye (1 mM ATP) and 20 μM dye (1.25 mM ATP), respectively. Myosin's $Mg^{2+}$ ATPase is only partially inhibited (50%) even at high dye concentrations (2 mM), with half-maximal inhibition occurring at 500 μM dye. Examination of the kinetics of inhibition reveals that the dye acts as a linear, mixed inhibitor, exhibiting both competitive and uncompetitive inhibition. Competitive binding predominates with a $K_i$ = 0.24 μM, and is stronger than that of the substrate. Uncompetitive binding by the dye is significantly weaker with $K_i'$ = 32.5 μM. Tension generation in fibers of rabbit psoas muscle is also completely inhibited by Cibacron Blue F3GA, upon pre-incubation with the dye. Half-maximal inhibition occurs at approx. 300 μM dye (5 min pre-incubation). Binding studies indicate that the dye inhibits S1 and HMM binding to myofibrils, 68% inhibition at 500 μM dye. Measurement of dye binding to myosin reveals that approx. 6 moles of dye bind per mole of myosin at 10 μM dye, 1 μM myosin.

Work supported by grants NSF BMS75-14793 and CVRI Fellowship HLO7192-01 (A.P.T.).

**T-PM-Po81** REMOVAL OF THE 18,000-DALTON LIGHT CHAIN OF MYOSIN FROM FROG MYOFIBRILS. J.G. Sarmiento* and M. Bárány, University of Illinois Medical Center, Chicago, 60612 (Spons. by L.H. Schliselfeld)

Removal of the 18,000-dalton or DTNB light chain (DTNB-LC) from frog myofibrils was investigated by treating them with DTNB (10 mM) and one of three chelators, EDTA, EGTA, or CDTA (2 mM). Subsequently, the myofibrils were treated with 10-15 mM DTT in an attempt to remove the bound thionitrobenzoate group. Treated myofibrils were compared to control myofibrils, treated in the absence of reagents. The total myofibrilar -SH content was measured, the $Mg^{2+}$ activated ATPase activity was determined in the presence of 0.1 mM $Ca^{2+}$ or 1 mM EGTA, and the ATPase activity was also determined in the presence of 10 mM $Ca^{2+}$. The DTNB-EDTA treatment resulted in greater than 90% removal of the DTNB-LC (determined by SDS-urea gel analysis), and the $Mg^{2+}$-activated ATPase activity exhibited a full loss in $Ca^{2+}$ sensitivity. However, the treated fibrils showed a decrease in -SH content indicating incomplete recovery of the modified cysteine residues. Furthermore, the $Ca^{2+}$ (10 mM) activated ATPase of the treated fibrils was elevated about 2-fold. The DTNB-EGTA treatment proved to be ineffective in removal of the DTNB-LC and the loss in $Ca^{2+}$ sensitivity was insignificant. The DTNB-CDTA treatment removed the DTNB-LC by >90%, similarly to the DTNB-EDTA treatment. However, the $Ca^{2+}$ sensitivity of the DTNB-LC depleted fibrils was maintained up to 69%. The -SH content of the treated and untreated fibrils was the same, although the $Ca^{2+}$ (10 mM) activated ATPase of the treated fibrils was somewhat enhanced. These data suggest that DTNB-LC may not be involved in conferring $Ca^{2+}$ sensitivity to frog myofibrils. (Supported by NS-12172 from NIH and MDA).

**T-PM-Po82** THE UNUSUAL MINIMUM IN SOLUBILITY OF PARAMYOSIN AS THE IONIC STRENGTH IS VARIED AT pH 7.00. L. B. Cooley and S. Krause, Rensselaer Polytechnic Institute, Troy, New York 12181.

Both native and partially degraded paramyosin from Mercenaria mercenaria exhibited a solubility minimum at pH 7.00 in the ionic strength range of 0.05 M to 0.07 M. At higher and at lower ionic strengths the solubility increases. This is in sharp contrast to the behavior exhibited by most proteins. In general a protein is insoluble in distilled water and its solubility increases as the ionic strength increases until a maximum in solubility is reached. At higher ionic strengths the protein is salted out. Alkali treatment which resulted in partial dephosphorylation of paramyosin affected the solubility at ionic strengths above 0.0 5 M, but not at lower ionic strengths. An explanation for the highly unusual solubility minimum is suggested based on charge interactions between paramyosin molecules. The model is supported by the results of pH titrations at ionic strengths below and above the ionic strength of the solubility minimum.

**T-PM-Po83** AGGREGATION OF MYOSIN AND LIGHT MEROMYOSIN IN THE PRESENCE OF CREATINE KINASE Stephen J. Koons and C. Richard Zobel, Dept. of Biophysical Sciences, State Univ. of N.Y., Buffalo, N.Y. 14214.

Dialysis of myosin into .14 M NaCl, 5 mM TES at pH 8.3 yields homogeneous aggregates that sediment with a sharp schlieren peak. Addition of small concentrations of creatine kinase (CPK) prior to dialysis causes the formation of large aggregates that sediment faster than myosin alone. Larger CPK concentrations progressively increase the sedimentation coefficient, while broadening the schlieren peak. At pH 8.3 a molar excess of CPK destroys the schlieren peak, while the peak vanishes at pH 7.5 in the presence of a 1:1 molar ratio of CPK to myosin. The absence of a sharp boundary indicates heterogeneous aggregation. Sedimentation of light meromyosin (LMM) with CPK in .2 M NaCl, pH 7.5 shows that CPK induces aggregation of LMM. Protein concentration determinations of the supernatants following preparative centrifugation of myosin-CPK and LMM-CPK mixtures in .15 M NaCl confirm that CPK binds to myosin and to LMM, and that myosin and LMM aggregate more heavily in the presence of CPK. The heterogeneous aggregation of myosin with CPK suggests that CPK binding to myosin is not likely related to the assembly of the M-line, even though CPK has been identified as an M-line constituent and binds to the LMM segment of myosin.

**T-PM-Po84** PHYSICAL CHEMICAL AND ENZYMATIC STUDIES ON RABBIT SKELETAL MUSCLE M-LINE PROTEINS, CREATINE KINASE AND THE 165,000 DALTON PROTEIN COMPONENT AND THEIR INTERACTION WITH EACH OTHER AND WITH MYOSIN AND MYOSIN SUBFRAGMENTS. R.S. Mani* and C.M. Kay, Medical Research Council of Canada Group in Protein Structure and Function, Department of Biochemistry, University of Alberta, Edmonton, Alberta, Canada T6G 2H7.

The M-line proteins, creatine kinase (CPK) and the 165,000 dalton protein component, were isolated from rabbit skeletal muscle using a low ionic strength extraction followed by DEAE-cellulose chromatography. Sedimentation equilibrium, circular dichroism (CD) and gel filtration chromatography were employed to establish a physical relationship between the M-line proteins and myosin and its subfragments. CD measurements indicated CPK to interact with myosin, heavy meromyosin (HMM) and heavy meromyosin subfragment 1 (HMM-S1). The $Ca^{2+}$ activated ATPase activities of myosin, HMM and HMM-S1 were inhibited by the addition of CPK. Sedimentation equilibrium studies gave a molecular weight of 205,000 for the CPK-S1 complex. Addition of 165,000 protein component of M-line lowered the enzymatic activity of CPK and the nature of the inhibition was competitive. The 165,000 protein component interacts with HMM-S2 and a molecular weight of 230,000 was obtained for this complex by the techniques of gel filtration chromatography and ultracentrifugal studies. A fragment of molecular weight 95,000 was isolated from the 165,000 M-protein by controlled chymotryptic digestion which also binds to HMM-S2. Interaction of the 165,000 protein component with the flexible hinge region of myosin may have special significance in terms of the mechanism accounting for the reversible expansion of the interfilament distance which occurs during contraction.

**T-PM-Po85** KINETICS OF CALCIUM BINDING TO WHITING PARVALBUMIN. Howard White, Dept. of Biochemistry, University of Arizona, Tucson, Arizona 85721 and Juliette Closset* Institut de Physique, Universite de Liege, Liege, Belgium.

Calcium binding shifts the fluorescence emission maximum of the single tryptophan residue of whiting parvalbumin from 340 to 325 nm and increases the intensity at the maximum 2.5 fold ($\lambda$ excitation = 290 nm). The fluorescence intensity at 325 nm increases linearly with the addition of calcium up to a maximum at two moles calcium per mole parvalbumin. The equilibrium constant of calcium binding, measured using calcium/EGTA buffers is $1.2 \times 10^6$ $M^{-1}$ and has a Hill coefficient of 2.0 in 100 mM KCl, 50 mM Tris, pH 8.0, 20° C. The kinetics of calcium binding was measured under indentical conditions from the increase in fluoresence ($\lambda$ excitation = 280 nm, $\lambda$ emission = 315 nm) observed upon mixing 40 μM parvalbumin with 10 mM calcium/nitrilotriacetate buffers (2 to 50 μM free calcium) in a stopped-flow fluorimeter. Calcium binding follows pseudo first order kinetics and is proportional to calcium concentration ($k = 1.4 \times 10^6$ $M^{-1}sec^{-1}$) up to a rate of at least 60 $sec^{-1}$. The rate of dissociation was determined by mixing calcium saturated parvalbumin with 0.1 to 10 mM EGTA or EDTA and found to be independent of chelator and chelator concentration. The rate of calcium dissociation was not a single first order process but could be described by two first order rate constnats of 2 and 5 $sec^{-1}$. A minimal mechanism consistant with the data is:

$$\text{Parvalbumin} + Ca \underset{2\ sec^{-1}}{\overset{1.4 \times 10^6\ M^{-1}sec^{-1}}{\rightleftarrows}} \text{Parvalbumin}\cdot Ca + Ca \underset{5\ sec^{-1}}{\overset{10^7\ M^{-1}sec^{-1}}{\rightleftarrows}} \text{Parvalbumin}\cdot Ca_2$$

**T-PM-Po86** $^1H$ NMR PROBES OF THE INTERACTION OF PARVALBUMIN WITH LANTHANIDES. L. Lee*, E.R. Birnbaum*[1] and B.D. Sykes, M.R.C. Group on Protein Structure and Function, Department of Biochemistry, University of Alberta, Edmonton, Canada T6G 2H7.

Calcium binding proteins play an important role in a number of biochemical processes. 270 MHz $^1H$ NMR studies indicate that the interaction of amino acids near the binding sites of parvalbumin with selected lanthanides such as ytterbium results in high resolution NMR spectra exhibiting a series of resonances with shifts as far downfield as 32 ppm and as far upfield as -19 ppm. These resonances are sensitive monitors of the geometry and behavior of the metal binding sites of proteins. Although the exact function of the parvalbumins is not known, they have been studied with the aim of developing a general technique to determine the structure of the metal ion binding sites in proteins. The X-ray crystallographic structure of parvalbumin is known to high resolution and serves to calibrate this probe. The spin lattice relaxation times and linewidths of the shifted resonances have been analyzed in terms of Solomon-Bloembergen and susceptibility relaxation to yield the distances from the metal ion to the nuclei whose resonances are shifted. The most downfield and upfield shifted resonances for parvalbumin + $Yb^{+++}$ at a 1:1 molar ratio arise, for example, from nuclei 4.8 Å and 5.2 Å, respectively, from the metal. The shifts can then be analyzed to ascertain the geometry of the residues around the metal binding site, with various parvalbumin isozymes aiding in the assignment of these resonances. The number of metal binding sites, the relative binding strengths for each site, and the order in which the sites are filled have been determined by titrations of the protein with the lanthanide ions. These techniques have also been used to estimate that the single $Ca^{++}$ binding site of the CB-9 fragment of TnC is on average ~25% less compact than the metal binding sites of parvalbumin.

[1]New Mexico State University, Department of Chemistry, Las Cruces, N.M. 88003.

**T-PM-Po87** THIN FILAMENT REGULATION AND HYBRID ACTOMYOSIN ATPase ASSAYS. J. Talbot* and R.S. Hodges, M.R.C. Group on Protein Structure and Function, Department of Biochemistry, University of Alberta, Edmonton, Canada T6G 2H7.

The proposed mechanism for the regulation of the actomyosin ATPase reaction of striated muscle is thought to exist at the level of the thin filament. It has been reported that the inhibition of skeletal muscle actomyosin ATPase is greater with skeletal muscle Tn-I than with cardiac muscle Tn-I while the situation is reversed with cardiac muscle actomyosin. The thin filament is composed of actin, the troponin complex and tropomyosin. In these assays α-Tm, which is found both in cardiac and skeletal muscle, was used. It has also been suggested on the basis of similar molecular weight, amino acid composition and peptide maps that actin from both striated muscle sources is highly similar if not identical. If they are identical then the only component of the thin filament left as a candidate for the differences in inhibition is the troponin. It is relatively easy to understand why the binding of troponin I, the inhibitor molecule, from a skeletal source would inhibit skeletal actomyosin ATPase more efficiently than Tn-I from cardiac muscle. It is then difficult to understand how with the same tropomyosin and actin as in the skeletal system, these Tn-I molecules now reverse their efficiency of inhibition of cardiac actomyosin unless the myosin is somehow involved. Evidence is presented using hybrid actomyosin ATPase systems that suggests the thin filament model of control may have to be extended. Furthermore, assays of synthetic peptides resembling the inhibitor regions of skeletal and cardiac Tn-I are reported and it is shown that they parallel the activity of their parent molecules.

**T-PM-Po88** INTERACTION OF PHALLOIDIN WITH PARTIALLY POLYMERIZED ACTIN. L.C. Gershman, L.A. Selden* and J.E. Estes. Medical and Research Services, U.S. V.A. Hospital, Albany, N.Y. and Department of Physiology, Albany Medical College, Albany, N.Y. 12208.

Phalloidin has been reported to promote the polymerization of actin and to stabilize its polymeric state (Dancker et al., Biochim. Biophys. Acta 400, 407 (1975)). Partially polymerized actin populations at equilibrium in 10 mM KCl at 25°C have a critical actin concentration, as determined by both viscosity measurements and their ability to activate the heavy meromyosin subfragment 1 ATPase activity, of 10 μM (Estes and Gershman, Biochemistry 17, 2495 (1978)), while similar actin populations containing equimolar phalloidin have a critical actin concentration less than 1 μM. When fully polymerized actin is diluted to a concentration of 10 μM in 10 mM KCl, the viscosity of the solution rapidly decreases to a value indicative of the presence of short polymers and nuclei, while its rate of proteolytic digestion remains low and linear with time. If fully polymerized actin in the presence of phalloidin is similarly diluted, only a small decrease in viscosity is observed, and the actin population is essentially indigestible. It thus appears that phalloidin stabilizes actin polymers by greatly reducing the rate of depolymerization. A similar effect, the stabilization of actin nuclei, is probably responsible for the moderate acceleration of actin polymerization observed in the presence of phalloidin.

Supported by NIH grants 1-RO1-AM21573 and T32-GM-07033.

**T-PM-Po89** G→F TRANSFORMATION OF ACTIN AT LOW IONIC STRENGTH INDUCED BY EGTA. N. Avissar*, E. Kaminsky*, S.J. Leibovich *† and A. Oplatka†. Beilinson Hospital, Petah Tikva and (†) The Weizmann Institute of Science, Rehovot, Israel.

Addition of 0.2-2.0 mM EGTA to rabbit skeletal G-actin in 5-10 mM phosphate or Tris buffer (pH 8.0) in the presence of 0.2 mM ATP caused increase in viscosity up to a level close to that reached by that in 50 mM KCl. Electron microscopy indicated the formation of filamentous actin which appears to be somewhat more flexible than F-actin obtained by polymerization with KCl. The effect of EGTA is probably due to chelation of $Ca^{2+}$ ions. When the ATP concentration was reduced to 0.01 mM or less, EGTA was incapable, while 50 mM KCl was still capable, of polymerizing the G-actin. It may be that ATP splitting is essential for the formation of filamentous actin by EGTA. The F-actin obtained at low ionic strength was depolymerized by DNAase I faster than KCl-polymerized actin. In conclusion, filamentous actin can be stable also in very low ionic strength media provided $Ca^{2+}$ ions are removed, whereas for G-actin to be the only form of the protein in such media, micromolar concentrations of $Ca^{2+}$ must be present.

T-PM-Po90 $^1$H NMR STUDIES OF RABBIT TROPOMYOSINS. B.F.P. Edwards and B.D. Sykes, M.R.C. Group on Protein Structure and Function, Department of Biochemistry, University of Alberta, Edmonton, Alberta, Canada T6G 2H7.

We have previously assigned the $^1$H NMR resonances of histidines 153 and 276 of rabbit αα tropomyosin and reported on their anomalous pH titration curves (B. Edwards and B. Sykes (1978) Biochemistry 17, 684). We have since determined that the cooperativity of the titration curves, which exhibit Hill coefficients approaching 2.0 at low ionic strength, is a result of the end-to-end polymerization which is known to be pH dependent. We had also observed that resonances from the two His 153 residues of αα or ββ tropomyosin broadened into an envelope of resonances during their titration. We have found that this broadening can be engendered by forming a disulfide crosslink between the two Cys 190 residues of αα tropomyosin or by labelling them with the carboxymethyl group. Both modifications disrupt the coiled-coil of tropomyosin sufficiently to create a series of conformations at His 153 of differing pKa values. Transfer of saturation experiments indicate that exchange among these conformations is very slow or non-existent. Labelling Cys 190 with the amidocarboxymethyl group does not broaden the resonances of His 153, indicating that the uncharged label is less disruptive. The relative temperature stabilities, monitored by circular dichroism, show that the amidocarboxymethyl derivative is slightly less stable than the fully reduced form, but is significantly more stable than carboxymethyl labelled αα tropomyosin. Moreover, ββ tropomyosin, which has two cysteines per chain, is destabilized by 10°C when labelled with the charged carboxymethyl group. We have also observed that crosslinking at Cys 190 perturbs the resonances of His 276 but to a lesser extent than those of His 153. If one assumes a coiled-coil rod-like structure for tropomyosin then the structural perturbation at Cys 170 is propagated 50 Å to His 153 and 120 Å to His 273.

T-PM-Po91 MODIFICATION OF CYSTEINE AND METHIONINE RESIDUES OF TROPOMYOSIN; EFFECTS ON POLYMERIZABILITY, BINDING TO ACTIN AND INHIBITION OF ACTO-HEAVY MEROMYOSIN ATPase. S. Wong*, T. Tao, and S.S. Lehrer, Dept. of Muscle Res., Boston Biomed. Res. Inst., Boston, MA 02114 and Dept. of Neurology, Harvard Medical School, Boston, MA.

Previous studies have shown that the introduction of an interchain S-S crosslink at Cys-190 of rabbit skeletal tropomyosin (Tm) affects the stability of its secondary and tertiary structure (J. Mol. Biol. (1978) 118, 209). The effects of similar modifications on other properties of Tm are now reported. Five different chemically modified Tm preparations were made: Tm reduced with dithiothreitol (red-Tm); red-Tm modified with N-ethylmaleimide (MalNEt-Tm); red-Tm modified with excess iodoacetamide (IA) at pH 7.5, 37°C, for 1½ hrs (IA-Tm); red-Tm whose SH groups were crosslinked by air oxidation ($O_2$-Tm); red-Tm whose SH groups were crosslinked by 5,5'-dithiobis(2-nitrobenzoate) ($Nbs_2$-Tm). Only in the case of IA-Tm, for which amino acid analysis showed that methionine as well as cysteine residues were modified, was there a substantial loss of polymerizability, loss of actin binding, and loss of inhibition of acto-heavy meromyosin ATPase. These results on IA-Tm differ from those of Johnson & Smillie (Biochemistry (1977) 16, 2264), who found that treatment of Tm with IA under acidic conditions caused a loss of polymerizability but not of actin binding. Our results indicate that 1) blocking or crosslinking of Tm's –SH groups does not greatly affect these properties of Tm; 2) modification of one or more methionine residues prevents end-to-end interaction, which may be necessary for the binding to actin and therefore for the inhibition of acto-heavy meromyosin ATPase. (Supported by NIH (AM-11677; HL-22461); NSF (GB 24316); and MDAA.)

T-PM-Po92 THE EFFECT OF $Mg^{2+}$ ON $Ca^{2+}$ BINDING TO THE $Ca^{2+}$-SPECIFIC SITES OF TROPONIN. James D. Potter and J. David Johnson, Department of Pharmacology and Cell Biophysics, University of Cincinnati College of Medicine, Cincinnati, Ohio 45267.

Several lines of evidence strongly support the idea that muscle contraction is regulated by $Ca^{2+}$ binding to the $Ca^{2+}$-specific regulatory ($Ca^{2+}$-R) sites and not by $Ca^{2+}$-binding to the $Ca^{2+}$-$Mg^{2+}$ sites of Tn. The most compelling evidence is the fact that $Ca^{2+}$ exchange with the $Ca^{2+}$-R sites is rapid enough to be involved in the contraction-relaxation cycle, whereas that with the $Ca^{2+}$-$Mg^{2+}$ sites is not (Johnson, Charlton, Potter, Biophys. J. 21, 105a, 1978). If only the $Ca^{2+}$-R sites of Tn are involved in regulation, then it is difficult to explain the shifts in the $Ca^{2+}$-dependence of tension development that have been seen as $[Mg^{2+}]$ is increased. Since most of these shifts were observed at relatively high $[Mg^{2+}]$, it is possible that the $Ca^{2+}$-R sites may bind $Mg^{2+}$ with a relatively low affinity and therefore was previously undetected. $Ca^{2+}$ binding to the $Ca^{2+}$-R sites as a function of $[Mg^{2+}]$ was followed by measuring the $Ca^{2+}$-dependence of $TnC_{DAN7}$ fluorescence in 2 mM EGTA, 10 mM $PO_4$ pH 7.0, and either 0, 5, 10 or 25 mM $MgCl_2$ at constant ionic strength by varying [KCl] from 90 mM to 15 mM. Increasing $[Mg^{2+}]$ lowered the affinity of the $Ca^{2+}$-R sites for $Ca^{2+}$ with a $K_{Mg}$ of 2 x $10^2$ $M^{-1}$. Studies are currently underway to demonstrate these effects in the absence of EGTA. Preliminary measurements on TnT-TnI-$TnC_{DANZ}$ suggest similar effects with increasing $[Mg^{2+}]$. Thus, these results could explain the shifts seen in the $Ca^{2+}$-dependence of tension development produced by increasing $[Mg^{2+}]$. JDP is an EI of the AHA, JDJ is a fellow of the MDA. Supported by AHA grants 75-818 and 78-1167 and NIH HL 22619 (IIIA).

**T-PM-Po93** SOLUTION CONFORMATION AND HYDRODYNAMIC PROPERTIES OF RABBIT SKELETAL TROPONIN-T. F. G. Prendergast and J. D. Potter, Dept. of Pharmacology, Mayo Foundation, Rochester, MN and Dept. of Pharmacology and Cell Biophysics, Univ. of Cincinnati College of Medicine, Cincinnati, OH 45267.

The solution conformation and hydrodynamic properties of rabbit skeletal troponin-T have been examined by analytical ultracentrifugation, gel exclusion chromatography and fluorescence spectroscopy. Because of the relative insolubility of troponin-T in aqueous media of low ionic strengths, experiments were performed in solutions of high ionic strength. Ultracentrifugal data suggest that in its native conformation, the molecule is elongated. Troponin-T is also excluded from Sephacryl S-200. Finally, fluorescence depolarization experiments also suggest a rod-like conformation for the molecule. Both troponin-T and tropomyosin are therefore similar in conformation and since these proteins are known to interact with each other, this similarity of form may have functional significance. Additionally, the rod-shaped conformation of troponin-T may be significant with respect to the structural organization of whole troponin. Supported by MDA-24 and the Mayo Foundation (FGP), and AHA M81167 (JDP). JDP is an Established Investigator of the American Heart Association.

**T-PM-Po94** STUDY OF THE STRUCTURE OF TROPONIN-C BY MEASURING THE RELATIVE REACTIVITY OF LYSINES WITH ACETIC ANHYDRIDE. S. E. Hitchcock and C. J. Zimmerman, Dept. of Biological Sciences, Carnegie-Mellon University, Pittsburgh, Pa. 15213.

A topological "map" of rabbit skeletal muscle troponin-C (TN-C) has been made by measuring the relative reactivities of the lysines with acetic anhydride in the native (0.1M NaCl, 0.01M TrisHCl, pH 7.5, 2mM $MgCl_2$, 0.5mM dithiothreitol, 0.1mM $NaN_3$) and unfolded states (6M GuHCl, 20mM triethanolamine, pH 9). Troponin-C, isolated and in complexes with troponin-I and troponin-T has been labeled in the native state, with and without calcium, with trace amounts of acetic anhydride (1 lysine in 400 is acetylated). Purified $^{3}H$-TN-C is combined with $^{14}C$-TN-C, labeled in 6M GuHCl, and is chemically labeled in 6M GuHCl. Following digestion with chymotrypsin and trypsin, the peptides are separated on columns and paper, and are located using autoradiography. The labeled peptides are eluted, counted for $^{3}H/^{14}C$, analyzed for amino acid composition and N-terminal residue. This allows identification of the peptides in the published sequence of Collins et al. (1977) and in the structure postulated by Weeds and McLachlan (1974). Using this procedure we have shown that lysine 20 (helical region) is the least reactive and lysines 37 (calcium binding region) and 153 (helical region) are the most reactive. The other six lysines have intermediate reactivities. There are no poorly reactive lysines indicating that none of these lysines is buried inside the protein. When TN-C binds to the other troponin components this overall pattern of relative reactivities appears to be retained. Similar studies of troponin-I and troponin-T are in progress. This research was supported by grants from the Muscular Dystrophy Association, National Institutes of Health (1 R01 AM19660) and Western Pennsylvania Heart Association.

**T-PM-Po95** THE SIGNIFICANCE OF HYDROPHOBIC FORCES IN TnC CONFORMATIONS, B.Nagy, University of Cincinnati Medical School, Cincinnati, Ohio 45267

Troponin C, (TnC), assumes a conformation with 36% $\alpha$-helix content (state I) measured as a CD spectrum of TnC + 1mM EDTA v.s. TnC + 1mM EDTA in 6M urea at pH 7.6 and 20°C. Binding of 2 $Ca^{2+}$/TnC cause a change of helix from 36 to 58% (state I + II); addition of 6M urea to 2Ca/TnC decreases the helix to 22% (state II), addition of 1mM EDTA to TnC of state I + II abolishes all of $\alpha$-helices (state III). Curve fitting analysis of the changes, was made, $\Delta[\Theta] = \Delta f([\Theta]_{H,\lambda,n} - [\Theta]_{R,\lambda})$ with two variables, helix (H) and random (R) in all wave lengths ($\lambda$), n=number of amino acids in helical segments, $\Delta f$ the fraction of amino acids changed. 5 segments are stabilized in $\alpha$-helix in state I, and 3 more segments became helical in state II. Since segments A,B,C,D,E,F,H contain more than 5 hydrophobic amino acid side chains (HAS) each, except G with 3 HAS and almost no HAS are in the connecting loops the main helix stabilizing factor both in state I and state II, appears to be HAS interactions within the turns of the helix. The HAS patches than contribute to intramolecular and inter subunit interactions. The small changes observed with binding to the low affinity sites (state IV) can tighten the binding loops which can cause enough movements of the HAS areas on the helical segments yielding a leverage for large movements of associated subunits.

Supported by MDA.